Quaternary Science Reviews 308 (2023) 108073

Contents lists available at ScienceDirect

Quaternary Science Reviews

journal homepage: www.elsevier.com/locate/quascirev

Visible or not? Reflection of the 8.2 ka BP event and the Greenlandian–Northgrippian boundary in a new high-resolution pollen record from the varved sediments of Lake Mondsee, Austria

Anna Schubert [a, **], Stefan Lauterbach [b, c, d], Christian Leipe [a, e], Achim Brauer [d, f], Pavel E. Tarasov [a, *]

[a] Institute of Geological Sciences, Paleontology Section, Freie Universität Berlin, Malteserstraße 74-100, Building D, 12249, Berlin, Germany
[b] Institute of Geography and Spatial Organization, Polish Academy of Sciences, ul. Twarda 51/55, 00-818, Warsaw, Poland
[c] Leibniz Laboratory for Radiometric Dating and Stable Isotope Research, Kiel University, Max-Eyth-Str. 11–13, 24118, Kiel, Germany
[d] GFZ German Research Centre for Geosciences, Section 4.3 – Climate Dynamics and Landscape Evolution, Telegrafenberg, 14473, Potsdam, Germany
[e] Domestication and Anthropogenic Evolution Research Group, Max Planck Institute of Geoanthropology, Kahlaische Str. 10, 07745, Jena, Germany
[f] Institute of Geosciences, University of Potsdam, Karl-Liebknecht-Str. 24–25, 14476, Potsdam, Germany

A R T I C L E I N F O

Article history:
Received 30 January 2023
Received in revised form
28 March 2023
Accepted 31 March 2023
Available online xxx

Handling Editor: Donatella Magri

Keywords:
European Alps
Lake sediments
Pollen and isotope records
Kretzschmaria deusta
Forest history
Archaeological cultures

A B S T R A C T

This paper presents a new pollen record from Lake Mondsee in the north-eastern European Alps and discusses changes in vegetation composition between 9000 and 7000 a BP in response to the 8.2 ka BP cooling event, which is clearly reflected in a stable oxygen isotope record from the same lake. Pollen and microcharcoal analyses performed at bi-decadal resolution provide detailed insights into the vegetation history and fire regime in the study area. The late Greenlandian and early Northgrippian between ca. 9000 and 8000 a BP were mainly characterised by the gradual expansion of spruce, accompanied by the retreat of hazel. Results of the pollen-based biome reconstruction show that the Greenlandian–Northgrippian boundary at ca. 8280 a BP was marked by a shift in the affinity scores of regional forest biomes, reflecting a decreasing role of temperate broadleaved trees and shrubs and a strengthening of boreal conifers in the study area. During the early Northgrippian between ca. 8000 and 7000 a BP, fir and beech spread around Lake Mondsee, which is in line with other pollen records from the northern Alpine Foreland, indicating cooler and moister conditions. This long-term trend is likely a response to decreasing summer insolation (i.e. decreasing summer temperatures) and the weakening of the Siberian High, which promoted westerly-driven moisture transport from the Atlantic region. Visual inspection of the Lake Mondsee pollen data does not reveal a clear signal of the 8.2 ka BP event. However, biomization results show a distinct minimum in the temperate deciduous biome scores and summed scores of plant functional types representing warm-loving tree and shrub taxa at ca. 8165–8135 a BP.

1. Introduction

Proxy-based reconstructions of past short-term (i.e. sub-decadal to century-scale) climate variability are of great interest, helping to (1) assess impacts of climate change on ecosystems, biodiversity and human communities at global and regional levels, (2) evaluate accuracy and predictive capacity of Earth system models, and (3) estimate vulnerabilities and limits of the natural world and human societies to adapt to climate change (Pörtner et al., 2022).

Among the century-scale climatic oscillations during the Holocene, the so-called '8.2 ka BP event' – an abrupt cooling that occurred approximately 8200–8000 calendar years before present (a BP, where BP stands for 1950 CE) – has attracted particular attention from geoscientists (e.g. Duan et al., 2021; González-Sampériz et al., 2009; Seppä et al., 2007; Veski et al., 2004), climate and vegetation modellers (e.g. Li et al., 2019; Morrill et al., 2014; Wiersma and Renssen, 2006) and archaeologists (e.g. García-Escárzaga et al., 2022; Griffiths and Robinson, 2018; Flohr et al.,

* Corresponding author.
** Corresponding author.
E-mail addresses: info@pollencounter.de (A. Schubert), slauterbach@leibniz.uni-kiel.de (S. Lauterbach), c.leipe@fu-berlin.de (C. Leipe), brau@gfz-potsdam.de (A. Brauer), ptarasov@zedat.fu-berlin.de (P.E. Tarasov).

https://doi.org/10.1016/j.quascirev.2023.108073
0277-3791/

2016; Schulting et al., 2022). Because of its outstanding position in the Holocene climate record, the 8.2 ka BP event has also been utilized for the formal subdivision of the Holocene epoch, defining the boundary between the Greenlandian age (Early Holocene sub-epoch) and the Northgrippian age (Middle Holocene sub-epoch) (Walker et al., 2019). First identified in a pollen record from the alpine valley Mesolcina in Switzerland (Zoller, 1960), the 8.2 ka BP cold oscillation has been recognised as the largest abrupt event of the past 12,000 years in the Greenland ice core records (Alley et al., 1997; Vinther et al., 2006), being characterised by pronounced cooling at a hemispheric scale (Kobashi et al., 2007). It is currently the most intensively studied and discussed climate excursion of the Holocene epoch (e.g. Parker and Harrison, 2022). Intensive research over the past two decades has resulted in a large body of papers identifying the 8.2 ka BP event in a variety of globally distributed proxy records, both marine and terrestrial (Morrill et al., 2013). To date, the most unambiguous and accurately dated reconstructions of the 8.2 ka BP event are provided by stable oxygen isotope records from ice cores and speleothems. Although pollen and other biological proxies from terrestrial archives (i.e. lake sediments and peat deposits) are the most abundant and reliable data (e.g. Finsinger and Tinner, 2007; Kleinmann et al., 2015; Lechterbeck and Rösch, 2021; Rey et al., 2013, 2017, 2020; Rösch et al., 2021), some of them suffer from insufficient temporal resolution and poor chronological control, which limits their use in discussions of timing, duration and magnitude of the 8.2 ka BP event (Parker and Harrison, 2022) and weakens the interpretation of its possible impact on regional vegetation and human environment (e.g. Schulting et al., 2022).

The abovementioned problems can be solved by using high-resolution pollen records from lake sediment records with very accurate chronologies established from counting of annual laminations, known as varves (e.g. Litt et al., 2009; Nakagawa et al., 2021; Schubert et al., 2020; Stebich et al., 2015). Such sedimentary archives covering the entire Holocene are relatively rare and their recovery and detailed analyses requires significant financial, labour and time investments (e.g. Brauer et al., 2014; Bronk Ramsey et al., 2012; Nakagawa et al., 2012). However, recent studies on varved lake sediments in different parts of Europe (e.g. Martin-Puertas et al., 2021; Rey et al., 2019, 2023; Zander et al., 2021) demonstrate the high potential of this approach for future research.

The freshwater Lake Mondsee situated in the Salzkammergut region (Upper Austria), ca. 25 km east of Salzburg at the northern margin of the European Alps (Fig. 1), is characterized by a complete Holocene and Lateglacial sediment succession (Lauterbach et al., 2011). Previous studies on a ~15-m-long composite sediment core (MO-05) from the southern part of the lake allowed to establish a robust chronology for the past 14.5 ka BP (Lauterbach et al., 2011) and emphasised a complex though sensitive response of aquatic and terrestrial proxies to climatic and environmental changes (Kämpf et al., 2014, 2015, 2020; Namiotko et al., 2015; Swierczynski et al., 2012, 2013a, 2013b). Andersen et al. (2017) examined the reflection of the 8.2 ka BP event in sediment core MO-05 by using sub-decadally resolved stable oxygen isotope ($\delta^{18}O$) data derived from the calcareous valves of benthic ostracods in the 1000-year interval between 8700 and 7700 a BP. Their study demonstrated a good agreement in timing, duration and magnitude of the 8.2 ka BP cooling in the Lake Mondsee record with other stable isotope

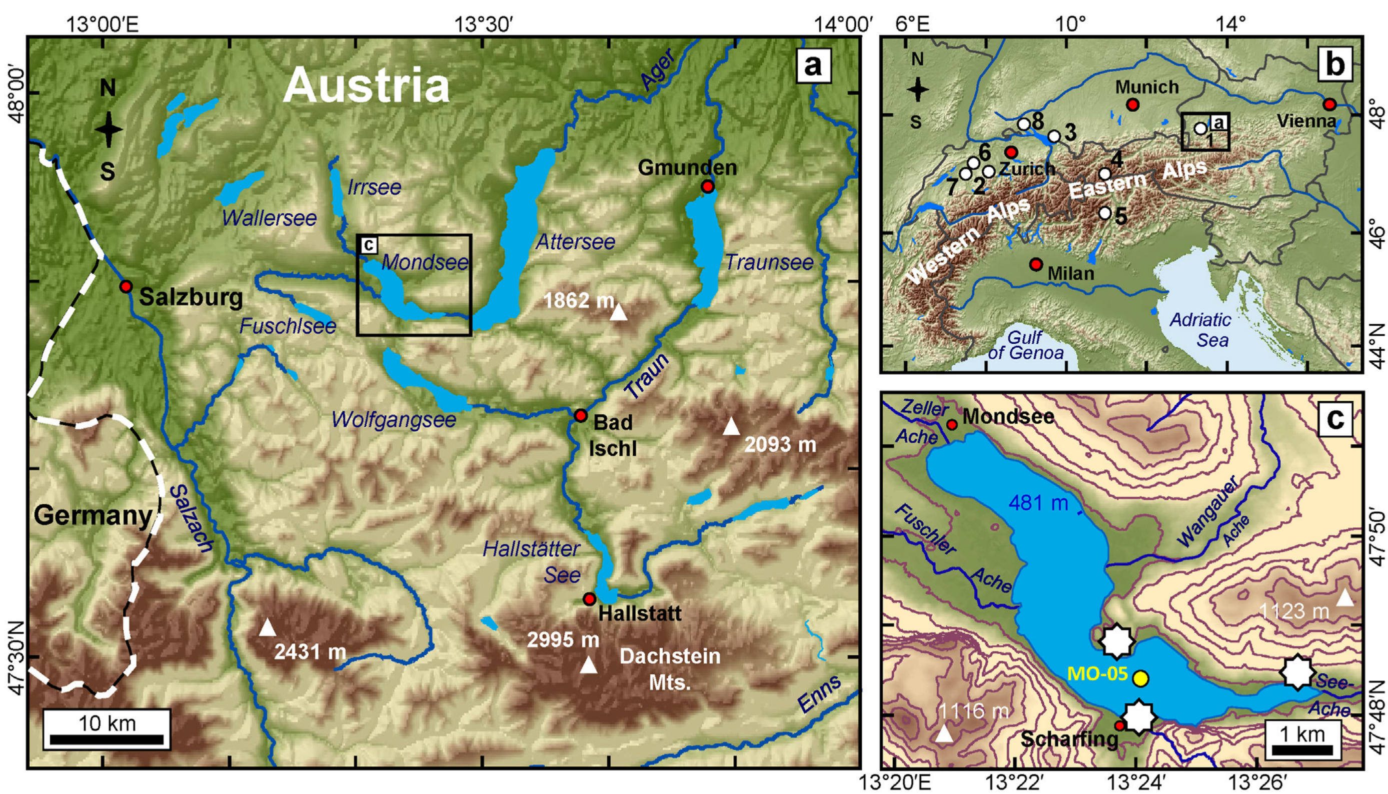

Fig. 1. Topographic maps showing (a) the Salzkammergut lake region in Upper Austria; (b) the location of the European Alps, the study region of Lake Mondsee (black rectangle) and other sites/areas with palaeoenvironmental records discussed in the text (numbered white circles: 1 – Lake Mondsee, 2 – Lake Soppensee, 3 – Lake Schleinsee, 4 – Lake Schwarzsee ob Sölden, 5 – Trentino, 6 – Lake Burgäschisee, 7 – Lake Moossee, 8 – Lake Litzelsee); and (c) Lake Mondsee with the locations of sediment core MO-05 (yellow point) and the three Neolithic pile-dwelling sites (white stars) (after Swierczynski et al., 2013a). The digital elevation models are based on 90-m-resolution Shuttle Radar Topography Mission (SRTM) v4.1 data (Jarvis et al., 2008). Modern state borders and the location of selected cities and villages (red dots) are provided for orientation.

records from Europe, but also provided evidence for a 75-year-long interval of increased air temperatures directly after the 8.2 ka BP event. Later, high-resolution palynological analyses performed for the interval 3450–1450 a BP in sediment core MO-05 allowed analysing the relationships between the pollen/vegetation composition, human habitation and regional climate variability on decadal and centennial time scales and revealed the high sensitivity of the dominant arboreal taxa to temperature fluctuations in the North Atlantic region and to moisture fluctuations controlled by changes in the strength of the Siberian High and the North Atlantic Oscillation (Schubert et al., 2020).

The archaeological sequence of the Salzkammergut lake district dates back to the Late Palaeolithic/Mesolithic period (e.g. Kern et al., 2009; Ruttkay et al., 2004; von Schnurbein, 2009; Wolf, 1977). The best dated and most famous cultures of the regional archaeological record, listed as UNESCO World Cultural Heritage, are the Late Neolithic Mondsee Culture, known for its pile-dwellings at the shores of Lake Mondsee and adjacent Lake Attersee (Kunze, 1986; Offenberger, 2012), and the Early Iron Age Hallstatt Culture (Kern et al., 2009), centred around Lake Hallstatt (or Hallstätter See; Fig. 1a). Archaeological investigations prove large-scale salt mining in the region since the Late Bronze Age, but earliest evidence for human activity in the area dates to ca. 7000 a BP (Kern et al., 2009). The transition from the Late Palaeolithic/Mesolithic (ca. 12,000–7550/7450 a BP) to the Early Neolithic (ca. 7550/7450–6850/6650 a BP) in the region is represented by the spread of the Linear Pottery Culture and agricultural practices. However, there is currently no archaeological evidence for permanent settlements in the Salzkammergut region prior to 7000 a BP (Kern et al., 2009) and the timing of the first agricultural activities remains ambiguous. However, three radiocarbon-dated lake-dwelling sites discovered by intensive archaeological work along the shorelines of the southern basin of Lake Mondsee (Fig. 1c) provide robust evidence for the local presence of Neolithic farmers since ca. 5800–5700 a BP (Swierczynski et al., 2013a). In the absence of archaeologically proven traces of human habitation and permanent settlements around Lake Mondsee during the time interval from ca. 9000 to 7000 a BP discussed in our study, the high-resolution palynological record should represent natural vegetation and allow to examine the effects of rapid climate changes around 8.2 ka BP on the regional terrestrial environments. On the other hand, identification of minor herbaceous pollen taxa (e.g. Cerealia type, *Plantago lanceolata*, *Urtica*, *Rumex*, Chenopodiaceae) and coprophilous fungi spores (e.g. *Sporormiella*, *Cercophora*, *Sordaria*) could provide important missing information on the early human impact, agricultural and animal grazing activities in the region (e.g. Rey et al., 2013, 2017; Rösch and Lechterbeck, 2016; Rösch et al., 2014, 2021; Schubert et al., 2020; Schwörer et al., 2015).

In the current paper, we present the detailed results of palynological and microcharcoal analyses on a 150-cm-long section of sediment core MO-05 from Lake Mondsee, spanning the interval from ca. 9000 to 7000 a BP. This interval covers an environmentally dynamic period of the Holocene Epoch prior to the Neolithic occupation of the catchment area, spanning the transition between the Greenlandian and the Northgrippian (i.e. between the Early and Middle Holocene) and the 8.2 ka BP cooling event. The newly generated records are then interpreted in terms of changes in vegetation composition, fire regime and potential early human impact and discussed in relation to regional and hemispheric-scale climatic changes.

2. Environmental setting

Lake Mondsee, the third-largest lake in the Austrian Salzkammergut lake district, is located at the northern margin of the European Alps (approx. 47°49′N, 13°24′E) at 481 m above sea level (a.s.l.). The lake is of glacial origin (van Husen, 1979; Kohl, 1998) and has a surface area of ~13.8 km^2, a catchment area of ~247 km^2 and a maximum water depth of ~68 m, which is reached in the southern part of the lake basin (Beiwl and Mühlemann, 2008). The northern, more shallow part of the lake is surrounded by the gently sloped hills of the Alpine Foreland, which are composed of Cretaceous siliciclastic sediments that are partly covered by Quaternary deposits, while the southern part of the catchment is dominated by the steep-sloped mountains of the Northern Calcareous Alps, which are mainly composed of Mesozoic limestones and dolomites (Irlweck and Danielopol, 1985; van Husen, 1989). The most important tributaries of Lake Mondsee are Fuschler Ache, Wangauer Ache and Zeller Ache (Fig. 1), which provide more than half of the inflowing water volume. The outflow stream Seeache connects Lake Mondsee with adjacent Lake Attersee (Fig. 1).

Lake Mondsee is located in the temperate oceanic climate zone (Geiger, 1954). The mean annual, July and January air temperatures at the Mondsee weather station (47.86°N, 13.35°E, 493 m a.s.l.) for the period 1971–2000 are +8.7, +17.8 and −0.5 °C, respectively. The average annual precipitation amounts to ~1550 mm (1971–2000), with one third of the total sum falling during the three summer months and the remainder being evenly distributed over the rest of the year (Central Institute for Meteorology and Geodynamics (ZAMG), Vienna, Austria). Heavy summer rains, often accompanied by thunderstorms, frequently cause severe flooding with enhanced supply of detrital catchment material by the tributaries, resulting in the formation of significant flood deposits in the lake (Swierczynski et al., 2012; Kämpf et al., 2014, 2015, 2020).

Today, ~52% of the catchment area are covered by forests while ~22% are covered by water, ~26% by meadows, pastures and arable land and <0.5% by buildings and commercial areas (Beiwl and Mühlemann, 2008). The elevated terrain (481–1700 m a.s.l.) and the complex topography of the Lake Mondsee catchment determine variable climatic conditions and the natural vegetation distribution along the altitudinal gradient. The natural vegetation near the lake is fragmentarily preserved. A unique beech (*Fagus*) forest with yew (*Taxus*), linden (*Tilia*), elm (*Ulmus*), willow (*Salix*), maple (*Acer*) and ash (*Fraxinus*) trees as well as numerous shrubs grows in the protected area “Pichlwald” in Loibichl at the eastern lake shore (Fuchs et al., 2004). It represents a temperate deciduous forest biome (Prentice et al., 1996) that is associated in the study area with the warmer zone, occupying lowlands and hills below 500 m a.s.l. Alder (*Alnus*) and birch (*Betula*) trees are common in the shore zone and in the floodplain forests. Species-rich mixed forests dominated by beech and spruce (*Picea*) and an admixture of oak (*Quercus*), fir (*Abies*), Scots pine (*Pinus sylvestris*), maple, ash, linden, alder, hazel (*Corylus*) and hornbeam (*Carpinus*) (Fuchs et al., 2004, 2005) are common in the altitudinal zone between 500 and 1000 m a.s.l. The altitudes between 1000 and 1600/1700 m a.s.l. are dominated by coniferous forests consisting of fir and spruce with an admixture of beech and few other cold-tolerant temperate deciduous trees. Above 1600/1700 m a.s.l., the subalpine zone of the Northern Calcareous Alps is occupied by larch (*Larix*) and stone pine (*Pinus cembra*) forests (Nationalpark, 2016).

3. Data and analytical methods

3.1. Core material and chronology

Within this study, we analysed a 150-cm-long section (840–990 cm composite depth) of the continuous sediment core MO-05 (Fig. 2a), which has been recovered in June 2005 from the deepest part of Lake Mondsee (Fig. 1c). MO-05 is 1493 cm long and covers the entire Holocene and Lateglacial (Lauterbach et al., 2011).

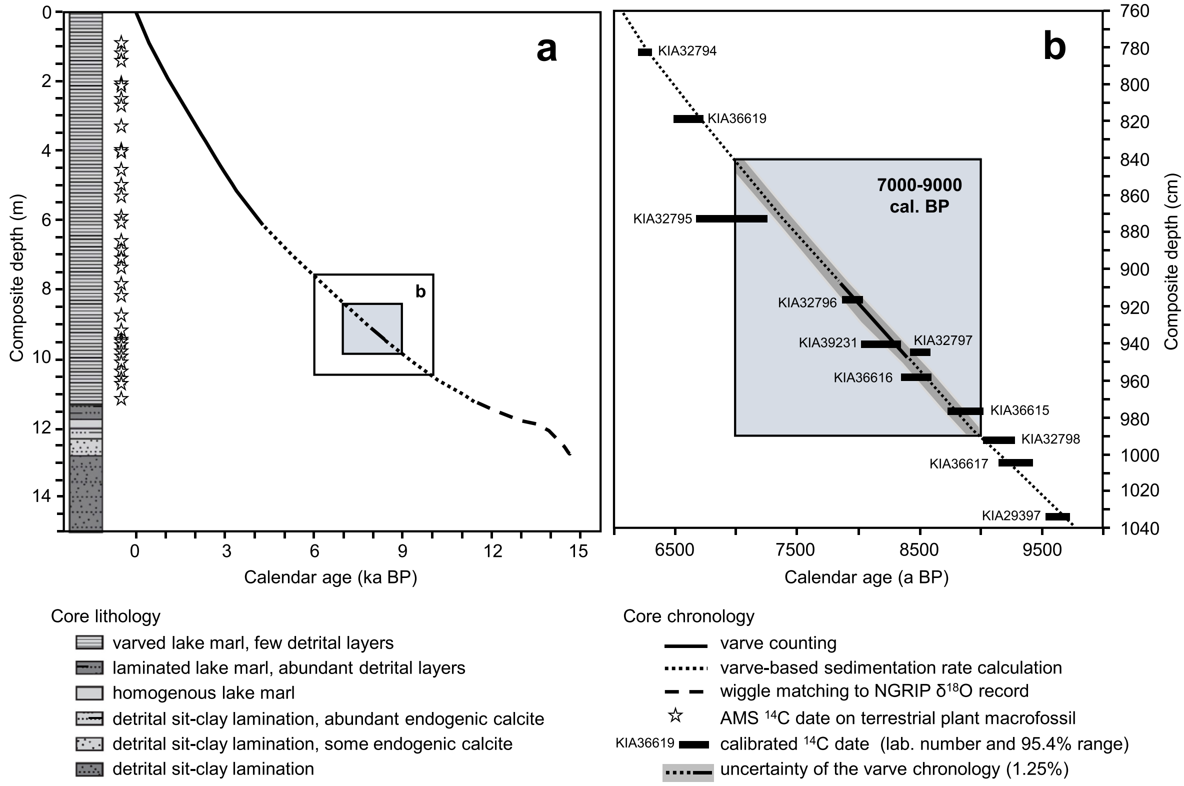

Fig. 2. (a) Schematic lithology and age model of sediment core MO-05 (modified from the electronic supplement to Lauterbach et al., 2011). Stars next to the lithological column indicate positions of terrestrial plant macrofossil samples that have been AMS ^{14}C-dated to support the varve counting-based Holocene chronology. The blue box between 840 and 990 cm composite depth indicates the interval between ca. 9000 and 7000 a BP investigated in this study. (b) Varve counting-based age model (black line) for the interval under investigation. The grey shading indicates the uncertainty of the varve chronology (1.25%; for details see Swierczynski et al., 2012, 2013b). Black horizontal bars indicate calibrated AMS ^{14}C dates (displayed are 95.4% ranges) of terrestrial plant macrofossil samples (see Table 1 for further details).

The chronology of its Holocene part (0–1129 cm composite depth) is based on continuous microscopic varve counting (0–608 and 909–947 cm composite depth) and a varve-based sedimentation rate chronology (608–909 and 947–1129 cm composite depth), supported by accelerator mass spectrometry (AMS) ^{14}C dates obtained from terrestrial plant macrofossils (e.g. Fig. 2; Table 1) as well as ^{137}Cs dating in the uppermost part (Lauterbach et al., 2011). As deduced from independent varve counts by two different examiners, the uncertainty of the MO-05 varve chronology is 1.25% (Swierczynski et al., 2012, 2013b). Following the published chronology (Andersen et al., 2017; Lauterbach et al., 2011), the section analysed in the current study covers the time interval between ~9000 and ~7000 a BP with an absolute age uncertainty of about ±100 years (Fig. 2b). All ages given in years (a) or kiloyears (ka) before present (BP) are varve/calendar years with BP referring to 1950 CE.

3.2. Palynological analysis and visualization of results

Palynological analysis was carried out on 78 sediment samples (1-cm-thick sediment slices, each incorporating 12–15 years) that were taken from sediment core MO-05 between 840 and 990 cm composite depth. The 2-cm sampling interval between analysed levels enables a temporal resolution of approximately 25 years.

Table 1

AMS ^{14}C dates obtained from terrestrial plant macrofossils from the Holocene part of the Lake Mondsee record (after Lauterbach et al., 2011) for the interval ca. 10,000–6000 calendar years before present (a BP). Italicised samples substantially deviate from the varve-based age model (Lauterbach et al., 2011). All conventional ^{14}C ages were calibrated using the OxCal v.4.4 software (Bronk Ramsey, 1995) and the IntCal20 calibration curve (Reimer et al., 2020).

Laboratory code	Composite depth (cm)	Dated material	Carbon content (mg)/δ^{13}C ± σ (‰)	AMS ^{14}C age (a BP ± σ)	Calibrated age (a BP, 95.4% probability)	Modelled calendar age (a BP)
KIA32794	782.25	leave fragments	1.04/−30.09 ± 0.15	5462 ± 36	6195–6310	6288
KIA36619	818.75	plant remains	1.65/−26.55 ± 0.13	5809 ± 36	6496–6729	6724
KIA32795	*873.00*	*plant remains*	*0.28/-32.70 ± 0.23*	*6088 ± 104*	*6678–7249*	7405
KIA32796	916.50	leave fragments	3.29/−29.61 ± 0.09	7129 ± 36	7868–8017	7985
KIA39231	941.00	twig	0.95/−29.41 ± 0.12	7349 ± 48	8024–8318	8312
KIA32797	*945.25*	*bark*	*5.11/-27.57 ± 0.07*	*7766 ± 35*	*8430–8600*	8368
KIA36616	958.75	plant remains	0.69/−25.24 ± 0.42	7631 ± 61	8342–8585	8556
KIA36615	977.00	plant remains	2.88/−30.85 ± 0.19	8019 ± 35	8724–9014	8817
KIA32798	993.00	bud scale	1.65/−25.73 ± 0.21	8192 ± 41	9019–9279	9049
KIA36617	1005.50	seed	4.66/−21.20 ± 0.34	8300 ± 32	9140–9430	9242
KIA29397	1034.75	seed	1.37/−23.89 ± 0.14	8638 ± 48	9529–9718	9697

Following the Sustainability Mission Statement adopted by the Freie Universität (FU) Berlin in research and teaching as well as EU regulations on the substitution of hazardous chemicals, we applied the extraction protocol described in Leipe et al. (2019) for the current study, avoiding both the use of HF and acetolysis. Chemical preparation of the wet sediment samples (~3 g) included treatment with cold 10% HCl to remove carbonates and hot 10% KOH to remove humic acids as well as dense media separation with sodium polytungstate (SPT) at a density of 2.1 g/cm^3 to remove siliceous matter. After SPT treatment, the sample residues were washed twice with distilled water and mounted in glycerol. The same approach has previously been successfully applied to Late Holocene sediments from the same sediment core, demonstrating excellent pollen recovery and preservation (Schubert et al., 2020).

In order to estimate pollen and non-pollen palynomorph (NPP) concentrations, one tablet of exotic *Lycopodium* spores was added to each sample (Lyco Batch No 1031: 20,848 ± 3457 spores per tablet) prior to chemical treatment (Stockmarr, 1971). Pollen of terrestrial and aquatic plants, fern and moss spores, some characteristic non-pollen palynomorphs (NPPs) and microcharcoal particles were counted using an Olympus CX31 light microscope at 400× magnification. Taxonomic identification was aided by published palynological keys and photo atlases (Beug, 2004; Demske et al., 2013; Moore and Webb, 1978; Reille, 1992, 1995, 1998; van Geel, 2001) as well as by the institute's reference collection. Ascospores of the parasitic fungus *Kretzschmaria deusta* (Type HdV-44) were identified after van Geel (1978) and van Geel et al. (2013). Microcharcoal particles (<200 μm in size) were counted as a fire proxy following Clark (1988) and Whitlock and Larsen (2001). Counted pollen sums vary between 600 and 869 terrestrial pollen grains per sample (667 on average). The counting of larger sums (>500 terrestrial pollen grains), also applied in a previous study (Schubert et al., 2020), has been demonstrated to reliably record rare (<1%) but indicative taxa (see Bennett and Willis (2001), Litt et al. (2009) and Weng et al. (2006) for further discussion) such as cool-temperate broadleaved evergreen *Hedera helix* (common ivy) and woody hemiparasitic *Viscum* (mistletoe) (Zagwijn, 1994). Individual taxa percentages for all terrestrial pollen taxa were calculated based on the sum of arboreal pollen (AP) and non-arboreal pollen (NAP) taken as 100%. Percentages for aquatic and spore-producing plant taxa and for non-pollen palynomorphs (NPPs) were calculated based on the terrestrial pollen sum plus the sum of palynomorphs in the corresponding group. The taxa percentage diagrams, which present the main analytical results employed in the discussion, were drawn using the software TILIA (Grimm, 1993, 2004).

3.3. Numerical analyses and data interpretations

For discussing the results and the potential impacts of major climatic forcings on changes in the pollen percentages of representative arboreal taxa (Fig. 5), we refer to the bioclimatic limits of plant functional types (PFTs), the definition of PFTs, the taxa-to-PFT and the PFT-to-biome assignment (Table 2) used in the BIOME global vegetation model based on plant physiology and dominance, soil properties and climate (Prentice et al., 1992) and in the European biome reconstructions from the late Quaternary pollen data (Prentice et al., 1996; Peyron et al., 1998; Tarasov et al., 1998). The calculation of biome scores for all analysed pollen samples was performed using an equation first published by Prentice et al. (1996). Consistently, a universal threshold pollen percentage of 0.5% was applied to all taxa in the biome-taxon matrix, as presented in that study. A square root transformation, aiming at amplifying the influence of minor pollen taxa, was then applied to pollen percentage values above zero.

The biome with the highest affinity score, or the one defined by fewer PFTs (when scores of several biomes are equal), should be assigned to each pollen spectrum (Prentice et al., 1996) and reflects a greater likelihood that this vegetation type grew close to the study site during the time of sample accumulation. The dominant biome reconstruction approach does not allow the reconstruction of transitional vegetation types; however, this important information can be obtained by examining the affinity scores of all biomes, which could be potentially present in the study region (e.g. Texier et al., 1997; Shumilovskikh et al., 2012; Kobe et al., 2020; Krikunova et al., 2022).

We used the total percentage of NAP as an indicator of landscape openness (e.g. Behre, 2007; Litt et al., 2009) and the microscopic charcoal particle content as a proxy for regional fire activity (Clark et al., 1989; Tinner et al., 1998; Whitlock and Larsen, 2001). *Kretzschmaria deusta*, commonly known as brittle cinder, is a fungus and plant pathogen found in temperate regions of the Northern Hemisphere. *K. deusta* is an indicator for intact late successional mixed beech and/or mixed oak forests as well as for flood events/soil erosion (van Geel et al., 2013). So far, the use of *K. deusta* as a climate proxy has not been sufficiently proven, but laboratory experiments demonstrate a relation between mycelium growth rate and air temperature (Cordin et al., 2021). These experiments revealed very slow mycelial growth at 10 °C compared to significantly higher rates at 15 and 20 °C and optimal growth at 25 °C (Cordin et al., 2021), but a possible impact of climate on the spread of the fungus is still difficult to assess. As detailed analyses performed on the same part of sediment core MO-05 do not suggest increased erosional input and/or more frequent flood events across the 8.2 ka BP event (Andersen et al., 2017), the *K. deusta* record generated in our study makes it possible to test its response to this climate oscillation.

4. Results

The microscopic analysis of the 78 samples used for this study revealed 82 identified taxa of palynomorphs, including 25 AP taxa (i.e. trees, shrubs and vines), 42 terrestrial NAP taxa (i.e. herbs and grasses), 5 aquatic plant taxa, 5 terrestrial cryptogam taxa (i.e. ferns

Table 2
Central European arboreal plant functional types (PFTs) with their characteristic taxa identified in the MO-05 pollen record (this study) assigned to the regional biomes (after Prentice et al., 1996). Biome and PFT abbreviations are given in brackets.

Plant functional type (trees and shrubs)	Taxa from the MO-5 record (this study) included	Regional biome
Boreal evergreen conifer (bec)	*Abies*, *Picea*, *Pinus cembra* (*i.e. Haploxylon* type)	Taiga (TAIG), Cool conifer forest (COCO), Cool mixed forest (COMX)
Boreal summer green (bs)	*Alnus*, *Betula*, *Populus*, *Salix*	TAIG, COCO, COMX, Temperate deciduous forest (TEDE)
Eurythermic conifer (ec)	*Juniperus*, *Pinus sylvestris* (*i.e. Diploxylon* type)	TAIG, COCO, COMX, TEDE
Temperate summer green (ts)	*Acer*, *Fraxinus* (*excelsior* type), *Quercus* (deciduous)	COMX, TEDE
Cool-temperate summer green (ts_1)	*Corylus*, *Fagus*, *Tilia*, *Ulmus*	COCO, COMX, TEDE
Warm-temperate summer green (ts_2)	*Fraxinus* (*ornus* type), *Rhamnus*, *Vitis*	TEDE
Cool-temperate broad-leaved evergreen (wte_1)	*Hedera*	TEDE
Heath (h)	Ericales	TAIG, COCO, COMX, TEDE

and mosses) and 5 taxa representing green algae and other NPPs (Supplemental Information Table 1). In total, only 18 terrestrial pollen taxa exceed 1% (Fig. 3a) while others are below this level (Fig. 3b). The recovery and preservation of all palynomorphs in the analysed samples were very good. Pollen concentration varied from 18,653 to 88,290 grains/g throughout the record with a mean value around 47,814 grains/g.

The summary palynological diagram (Fig. 3) shows that AP is predominant in the pollen assemblages throughout the record and varies between 88 and 96% (mean value ~93%). The NAP is dominated by Poaceae (grass) and Cyperaceae (sedge) pollen and shows a slight decrease in percentage values from the bottom (10–12%) to the top (4–6%) of the record. In the lower part of the record (990–939 cm), which represents the age interval prior ca. 8280 a BP, the temperate deciduous taxa *Corylus* and *Ulmus* are the most abundant, averaging at about 22 and 15% of the total pollen sum, respectively. Other representative deciduous taxa are *Quercus* and *Tilia*, followed by *Betula* and *Alnus*. *Picea* and *Pinus* predominate among the coniferous taxa (on average ~13 and ~8%, respectively). The *Corylus* and *Picea* percentage curves show an opposite trend, i.e. a decrease and an increase, respectively (Fig. 3a). In the middle part of the record (939–849 cm; ca. 8280–7100 a BP), *Picea* (on average ~24%) becomes the most dominant taxon, followed by *Ulmus* (~14%) and *Corylus* (~13%). *Fagus* and *Abies* start to appear regularly and *Pinus cembra* (stone pine) reaches up to 2%. The uppermost part of the record (849–840 cm; ca. 7100–7000 a BP) demonstrates a noticeable decrease in the average values of *Picea* (~11%) and *Ulmus* (~7%) and a corresponding increase in *Corylus* (23%). *Alnus*, *Fagus* and *Abies* reach their highest values in the record, i.e. 17%, 4% and 1%, respectively. All aquatic taxa (*Myriophyllum*, *Nuphar*, *Nymphoides*, *Sparganium* and *Typha latifolia* type) are minor pollen contributors and their total sum does not exceed 0.9% throughout the entire record. Spores of Polypodiales and *Pteridium* are the main contributors among the terrestrial cryptogams (Fig. 3a). In the NPP group, the green algae *Botryococcus* and fungal spores of *Glomus* and *K. deusta* as well as microcharcoal particles show the highest percentages and concentration values (Fig. 4).

The quantitative pollen-based biome reconstruction (Fig. 5) approves the subdivision based on the visual inspection of the pollen diagram (Fig. 3). The results show that the forest biomes, particularly cool mixed (COMX), temperate deciduous (TEDE) and cool conifer (COCO) forests, have the highest affinity scores. The species rich COMX biome dominates throughout the entire investigated section. In the lower (990–939 cm) and uppermost (849–840 cm) parts of the record, it is followed by the TEDE biome, while in between (939–849 cm) the COCO and TEDE biomes share the second/third places. The evergreen conifer forest biome (i.e. mountain taiga; TAIG) also shows relatively high scores in this interval. This is mainly due to a relative increase in the proportion of boreal evergreen conifer (bec) taxa and a less pronounced decrease in the proportion of broadleaved taxa contributing to the temperate summer green (ts) and cool-temperate summer green (ts_1) PFT, respectively (Fig. 5).

5. Discussion

5.1. Vegetation change and climate dynamics between 9000 and 7000 a BP

Pollen analysis has proven to be as a powerful tool to reconstruct changes in local to regional vegetation communities through space and time (e.g. Berglund and Ralska-Jasiewiczowa, 1986; Dimbleby, 1985; Fægri and Iversen, 1989). The analysis performed in the current study provides a very detailed and robustly dated record of vegetation changes around Lake Mondsee at the northern margin of the Austrian Alps across the Early to Middle Holocene (Greenlandian–Northgrippian) boundary. The late Greenlandian part of the investigated interval (ca. 9000–8280 a BP) reveals the dominance of species-rich COMX and TEDE forest communities with hazel, elm, linden, oak, ash, birch and alder at lower elevations and around the lake, while spruce and pine were characteristic elements of the COCO and TAIG biomes at higher elevations (Figs. 5 and 6a). Relatively low proportions of NAP (Fig. 6b) suggest that open vegetation played a minor role in the generally forested landscape and was probably confined to the lake shores. Generally low NAP percentages (i.e. below 10%) between 9000 and 7000 a BP were also observed in high-resolution pollen records from Switzerland and Germany (e.g. Litt et al., 2009; Rey et al., 2013; Tinner and Lotter, 2006), suggesting that the entire region north of the Alps was forested, although forest composition and canopy density likely varied from site to site and between lowland sites (e.g. Litt et al., 2009; Rey et al., 2017, 2020; Tinner and Lotter, 2006) and subalpine sites (e.g. Rey et al., 2013, 2022). Relatively high amounts of *Corylus avellana* pollen in the Lake Mondsee record (Fig. 3a) may indicate a relatively open mixed oak forest near the lake. In comparison, the pollen record from Lake Burgäschisee on the Swiss Plateau (Fig. 1b) reveals high percentages of temperate trees and shrubs between 9000 and 7000 a BP with a predominance of mixed elm-linden-maple-oak forests without spruce and a significant but gradually decreasing proportion of hazel (Rey et al., 2017).

The proportion of herbaceous pollen in recent sediments from Lake Mondsee is 17–19%. This corresponds to a satellite-based estimate of forest cover of 69% within a 15 km radius around the lake (Schubert et al., 2020) derived from the AVHRR modern tree cover dataset (DeFries et al., 2000). The main differences in the composition of the Early Holocene (i.e. late Greenlandian) vegetation at Lake Mondsee are the absence of beech, which contributes 8.4% to the modern pollen assemblage, as well as hornbeam, fir and yew. In addition, the contribution of hazel (2.8%), oak (1.5%), ash (1.7%), linden (0.2%) and elm pollen is significantly lower in the modern pollen assemblage, while the contribution of spruce (28.7%) and pine pollen (19.9%) is higher. Although, coniferous tree species (mainly spruce) are naturally predominant in the modern Austrian forests (i.e. 63.5% of the total forest area), this has been reinforced to some extent by human activities for economic reasons (Quadt et al., 2013).

Changes in pollen composition that began during the late Greenlandian continued during the early Northgrippian (ca. 8280–7000 a BP), indicating corresponding changes in regional vegetation. Thus, the continuing decrease in the percentages of herbaceous pollen (Fig. 6b) may reflect the further spread of forest vegetation or/and a higher density of the forest canopy. The decrease in the proportion of hazel (Fig. 6d), a typical edge and understorey species in open mixed deciduous forests (San-Miguel-Ayanz et al., 2016), and the increase in the proportion of shady boreal conifers (Fig. 5), mainly spruce (Fig. 6c), support this interpretation and explain the strengthening of the TAIG and COCO biomes (Fig. 5) in the study area during this interval. The early Northgrippian part of the MO-05 record also reveals the arrival (at ca. 7925 a BP) and successive spread of beech and fir (Fig. 6e).

The shade-tolerant and mesophytic end-successional species *Fagus silvatica* and *Abies alba* are important components of contemporary European forests (San-Miguel-Ayanz et al., 2016) and Holocene pollen records from Central Europe (Tinner and Lotter, 2006), including the Lake Mondsee area (Draxler, 1977; Schmidt, 1981; Schubert et al., 2020). Their arrival time and expansion patterns in different parts of Europe have been studied and discussed over the past decades (e.g. Magri et al., 2006; Tinner

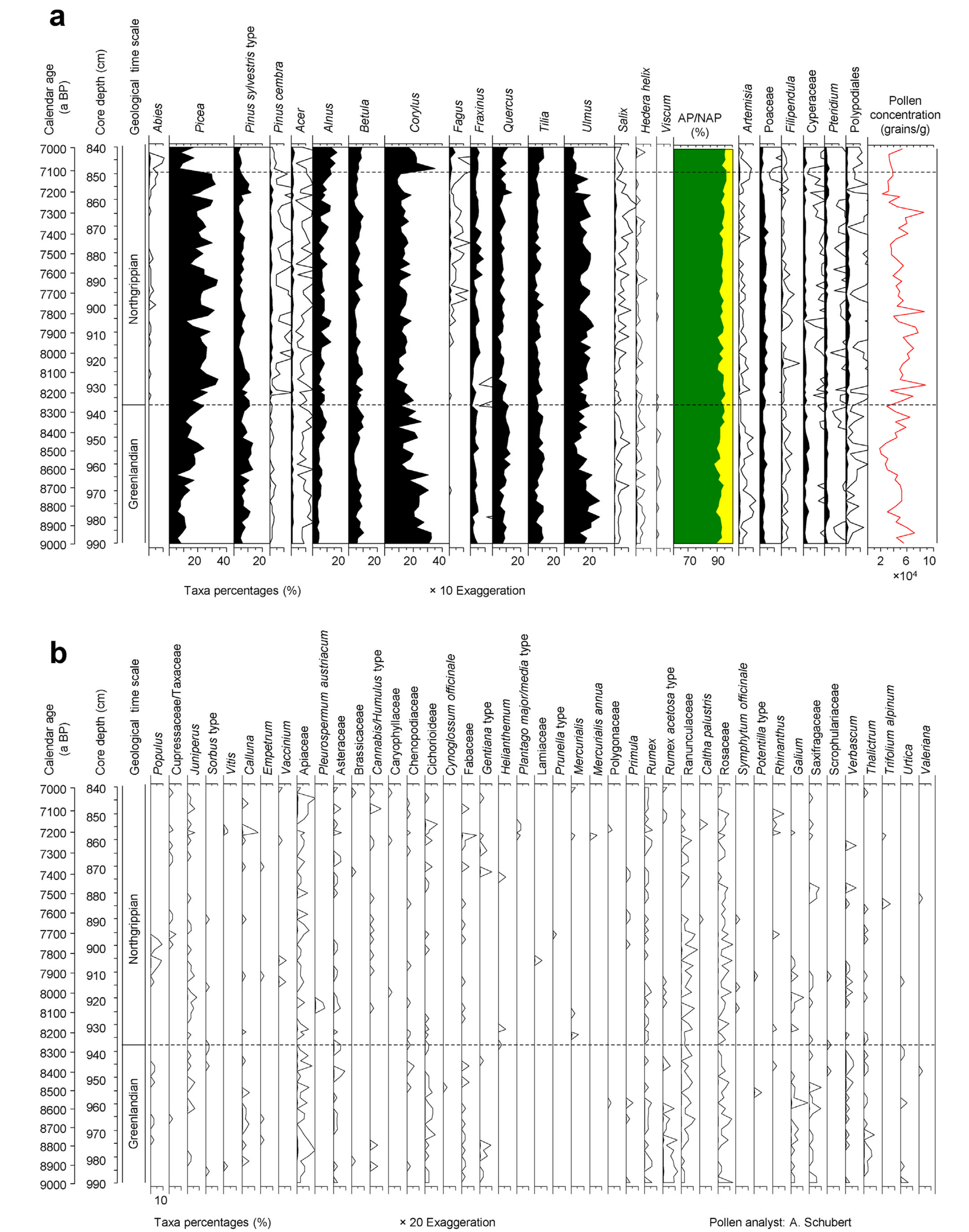
a
Calendar age (a BP)
Core depth (cm)
Geological time scale
Northgrippian
Greenlandian
Abies
Picea
Pinus sylvestris type
Pinus cembra
Acer
Alnus
Betula
Corylus
Fagus
Fraxinus
Quercus
Tilia
Ulmus
Salix
Hedera helix
Viscum
AP/NAP (%)
Artemisia
Poaceae
Filipendula
Cyperaceae
Pteridium
Polypodiales
Pollen concentration (grains/g)
×10^4
Taxa percentages (%)
× 10 Exaggeration
b
Calendar age (a BP)
Core depth (cm)
Geological time scale
Northgrippian
Greenlandian
Populus
Cupressaceae/Taxaceae
Juniperus
Sorbus type
Vitis
Calluna
Empetrum
Vaccinium
Apiaceae
Pleurospermum austriacum
Asteraceae
Brassicaceae
Cannabis/Humulus type
Caryophyllaceae
Chenopodiaceae
Cichorioideae
Cynoglossum officinale
Fabaceae
Gentiana type
Helianthemum
Plantago major/media type
Lamiaceae
Prunella type
Mercurialis
Mercurialis annua
Polygonaceae
Primula
Rumex
Rumex acetosa type
Ranunculaceae
Caltha palustris
Rosaceae
Symphytum officinale
Potentilla type
Rhinanthus
Galium
Saxifragaceae
Scrophulariaceae
Verbascum
Thalictrum
Trifolium alpinum
Urtica
Valeriana
Taxa percentages (%)
× 20 Exaggeration
Pollen analyst: A. Schubert

and Lotter, 2006; Giesecke et al., 2007; Kleinmann et al., 2015; Rey et al., 2017, 2020; Rösch and Lechterbeck, 2016; Rösch et al., 2014, 2021). However, the discussion of migrational leads and lags and their underlying drivers is often hampered by chronological uncertainties of the pollen records. Therefore, robustly dated records with chronologies established by varve counting and AMS ^{14}C dating on terrestrial plant remains are especially important. The timing of the spread of *Fagus* and *Abies* inferred from the new Lake Mondsee pollen record (Fig. 6e) is in good agreement with evidence from high-resolution pollen records from Lake Soppensee on the Swiss Plateau (Fig. 1b) and Lake Schleinsee (Fig. 1b), situated ~4 km northeast of Lake Constance (Tinner and Lotter, 2006), confirming a more or less synchronous onset of the expansion of *Fagus* and *Abies* in the northern Alpine Foreland during the early Northgrippian. However, the very detailed and well-dated pollen record from Lake Moossee (Fig. 1b) suggests that the local establishment of the first stands of *Abies alba* and *Fagus sylvatica* on the Swiss Plateau occurred at 8400 and 8200 a BP, respectively (Rey et al., 2020), i.e. earlier than around Lake Mondsee.

To date, there is no archaeological evidence of Neolithic occupation and land use in the Lake Mondsee area between 9000 and 7000 a BP. By reviewing lake sediment pollen records from southwestern Germany in terms of changes in vegetation and human impact Rösch et al. (2021) concluded that Neolithic human impact in the northern Alpine Foreland is generally characterised by increased amounts of microcharcoal and indicator taxa of human impact such as ruderals, apophytes (e.g. *Artemisia*, *Plantago lanceolata*) and Cerealia pollen although the NAP contribution may remain low. The MO-05 pollen record (Fig. 3), however, does not reveal similar evidence for human impact during the investigated time interval. In particular, Cerealia and *P. lanceolata* pollen grains as well as coprophilous fungi spores are absent, while other potential indicator taxa are either represented by single pollen grains only (e.g. *Urtica*, *Rumex*, Chenopodiaceae) or appear in very small numbers throughout the record (e.g. *Artemisia*). The data synthesis by Rösch et al. (2021) also suggests that between 7500 and 6300 a BP the lacustrine pollen records from the northern Alpine Foreland, far distant from the settlement areas of the Linear Pottery Culture, show little human impact. This is in agreement with the pollen record from Lake Burgäschisee (Fig. 1b), where the first pollen grains of Cerealia and *P. lanceolata* appear at ca. 6500 a BP, marking the onset of noticeable agricultural activities around the lake (Rey et al., 2017). The pollen record from Lake Litzelsee (Fig. 1b) in the western Lake Constance region (Rösch and Lechterbeck, 2016) also does not show any signs of significant human impact between 7500 and 7000 a BP, i.e. the time corresponding to the Linear Pottery Culture period, but, however, reveals a distinct rise in the charcoal contents.

Reviewing the vegetation dynamics in the northern Alpine Foreland between ca. 8700 and 7500 a BP, Tinner and Lotter (2006) concluded that neither human nor fire disturbance substantially promoted the expansion of *Fagus* and *Abies* in the regional forests during that interval. The microscopic charcoal record from sediment core MO-05 (Fig. 6f) is in line with these data, suggesting that regional fire activity was rather heterogeneous. At Lake Soppensee charcoal influx increased markedly after 8200 a BP, with peaks at 7985, 7685 and 7565 a BP. At Lake Schleinsee very high amounts of charcoal were accumulated at 8330 a BP and secondary peaks occurred at 8250 and 7950 a BP (Tinner and Lotter, 2006). Rey et al. (2017) reported an increasing trend in charcoal values at Lake Burgäschisee after ca. 7500 a BP, suggesting higher regional fire activity that peaked around 6500–5000 a BP, most likely in response to human activities such as slash-and-burn. In comparison, the only notable peak in charcoal concentration in the Lake Mondsee record dates to 7890 a BP. Given that charcoal concentrations were low during the rest of the study interval, this is consistent with the absent archaeological and palynological evidence for human impact in the area. Whether the fire event at 7890 a BP was caused by an accidental human visit or was of natural origin remains unresolved.

The hypothesis that 'native vegetation is the best expression of climate' (Köppen, 1923) has been validated on a global and large regional scale (e.g. Geiger, 1954; Prentice et al., 1992; Woodward, 1987). A recent comparison of the decadal- and century-scale variability in the MO-05 pollen record between ca. 3500 and 1500 a BP with Greenland ice core palaeoclimate records (Mayewski et al., 1997, 2004; Svensson et al., 2008) revealed a very high sensitivity of the vegetation in the study area to temperature and moisture variability in the North Atlantic region as well as to the intensity of the Siberian High (Schubert et al., 2020). Because of the absence of archaeological traces and the lacking palynological evidence for human activity around Lake Mondsee between ca. 9000 and 7000 a BP, climatic forcing of the observed vegetation changes can be considered more likely than an anthropogenic influence.

The most notable feature of the MO-05 pollen record (Fig. 4) and the pollen-based reconstruction of the vegetation around Lake Mondsee (Fig. 5) during the study interval is the shift in the affinity scores of regional TEDE and COCO forest biomes (Fig. 6a), reflecting a decreasing role of temperate broadleaved trees and shrubs (Table 2) and a strengthening of boreal conifers in the catchment area at the Greenlandian–Northgrippian boundary at about 8280 a BP. However, this change was preceded by a long-term gradual decline of *Corylus* (Fig. 6d) and the parallel gradual expansion of *Picea* in the study area (Fig. 6c). A similar trend in the *Corylus* pollen curve in high-resolution pollen records from the northern Alpine Foreland of Switzerland and Germany has previously also been interpreted in terms of climate change (Tinner and Lotter, 2006).

The interval between 9000 and 7000 a BP in the Northern Hemisphere mid-latitudes was characterised by decreasing but still higher-than-present (i.e. close to the Holocene maximum) summer insolation and increasing but lower-than-present winter insolation (Laskar et al., 2004). At 9000 a BP, the global sea level was ~20–25 m lower than today (Waelbroeck et al., 2002; Yokoyama et al., 2007). In the following, it quickly rose, reflecting melting of the Northern Hemisphere ice sheets (e.g. Stroeven et al., 2016; Margold et al., 2018), and reached ~5 m below modern levels at about 7000 a BP. In the European mid-latitudes, these boundary conditions should have led to warmer summers and colder winters (i.e. greater seasonality), higher evaporation and lower moisture availability, especially pronounced around 9000 a BP (Kutzbach and Webb, 1993). However, reconstructions of the Early Holocene climate based on over 500 pollen records from Europe show major spatial and seasonal differences in temperature trends (Davis et al., 2003), demonstrating the importance of regional studies.

A high-resolution chironomid-based mean July temperature reconstruction from Lake Schwarzsee ob Sölden (Fig. 1b) in the Eastern Alps (Ilyashuk et al., 2011), ~200 km southwest of Lake Mondsee, reveals that the Early Holocene summer climate was much warmer than today. Mean July temperatures were 2–4 °C higher until 8280 a BP but notably decreased thereafter (Fig. 6g). This is consistent with the decreasing trend in summer insolation

Fig. 3. Summary diagrams showing the relative abundance of representative arboreal pollen (AP), non-arboreal pollen (NAP) and spore taxa representing terrestrial vegetation in the analysed section of sediment core MO-05 from Lake Mondsee on depth and age scale (this study).

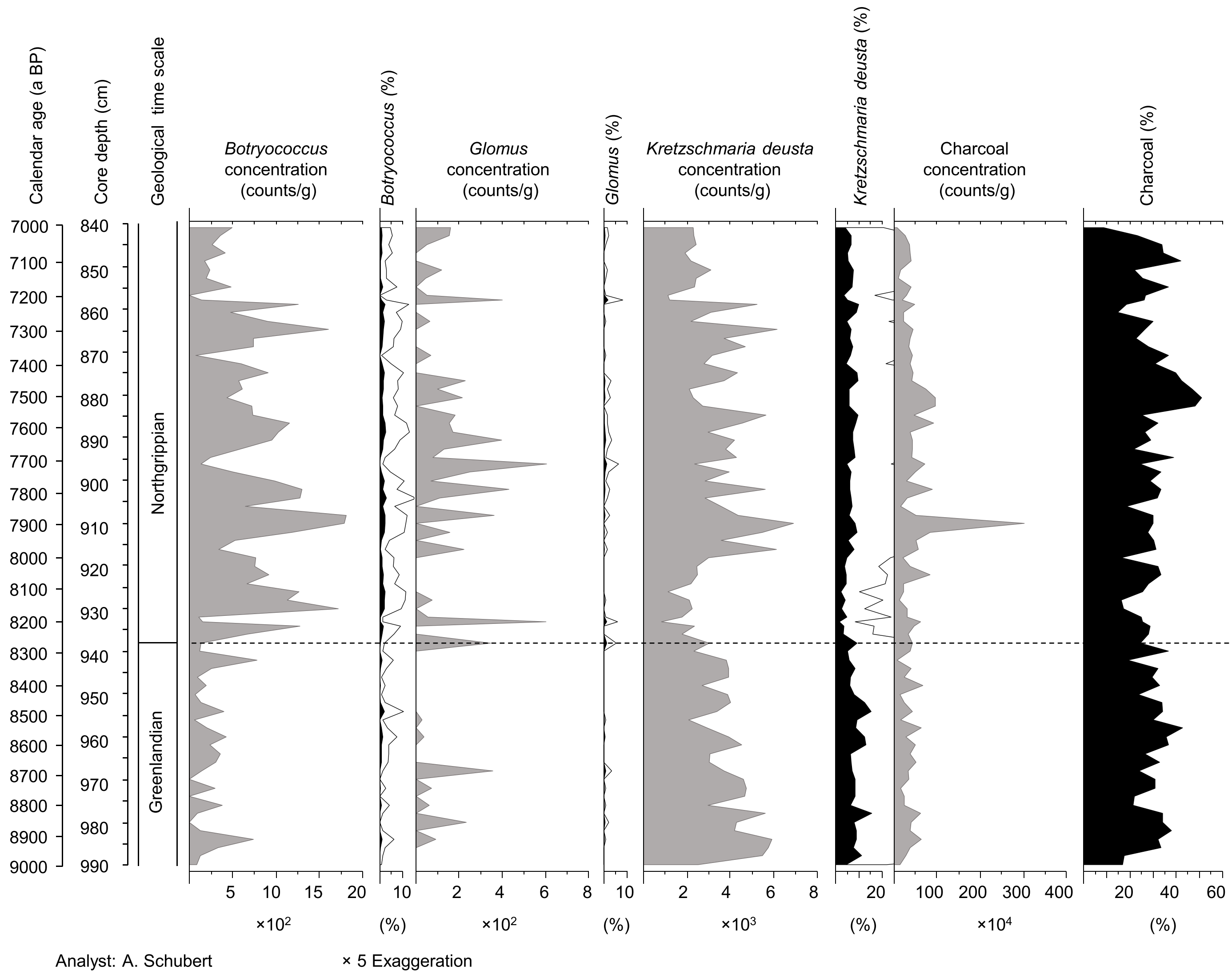

Fig. 4. Simplified diagram showing the relative abundance and concentration values of representative non-pollen palynomorph (NPP) taxa in the analysed section of sediment core MO-05 from Lake Mondsee on depth and age scale (this study).

and helps to explain gradual changes in the MO-05 pollen record (Fig. 3) and the reconstructed biomes (Fig. 6a). Tinner and Lotter (2006), by interpreting changes in several well-dated vegetation records from the western Alps, suggested that the decrease in summer temperatures after ca. 8300 a BP was accompanied by a marked increase in moisture supply. This interpretation is supported by evidence for regionally higher lake-levels and a positive hydrological balance at that time (Magny, 2004). Earlier, Magny et al. (2003) hypothesized that improved moisture conditions in Central Europe could reflect variations in the strength of the Atlantic Westerly Jet in relation with the thermal gradient between high and low latitudes. In the current study, lower percentages of *Picea* (Fig. 6c) and higher NAP values (Fig. 6b) during the late Greenlandian correspond to a stronger Siberian High (Fig. 6h; Mayewski et al., 1997, 2004) and higher than present regional summer temperatures (Fig. 6g), indicating a more continental and relatively dry climate regime. Higher *Picea* and lower NAP percentages during the early Northgrippian correspond to a weaker Siberian High accompanied by cooler summers, resulting in a less continental and relatively humid regional climate. Multiproxy records from lake sediments from the Baikal region (Kobe et al., 2020, 2022) also indicate a weakening of the strong winter anticyclone during the Early Holocene, which blocked the westerly flow and caused dry winter conditions in this region (Kleinen et al., 2011). In contrast, the following Middle Holocene experienced much faster forest expansion and a strengthening of the westerly circulation, which brought precipitation to the mid-latitudinal zone of Eurasia, stretching from France (Magny, 2004) and Germany (Litt et al., 2009) in the west to the Altai Mountains and the Lake Baikal region in the east (Kleinen et al., 2011; Tarasov et al., 2017).

The TEDE biome scores rise again above the COCO biome scores in the uppermost part of the investigated interval around 7100–7000 a BP (Fig. 6a). This change is associated with an abrupt decrease in *Picea* in the MO-05 pollen record (Fig. 3), accompanied by a short-term increase in *Corylus* percentages. However, neither very low NAP values (Fig. 6b) nor relatively constant scores of the temperature sensitive ts PFT (Fig. 5) indicate a significant decrease in atmospheric precipitation or temperature. The chironomid-based summer temperature reconstruction from Lake Schwarzsee ob Sölden (Fig. 6g) also shows rather low mean July temperatures during this period, suggesting another driving force behind the recorded changes in *Picea* and *Corylus*. Quadt et al. (2013) reported

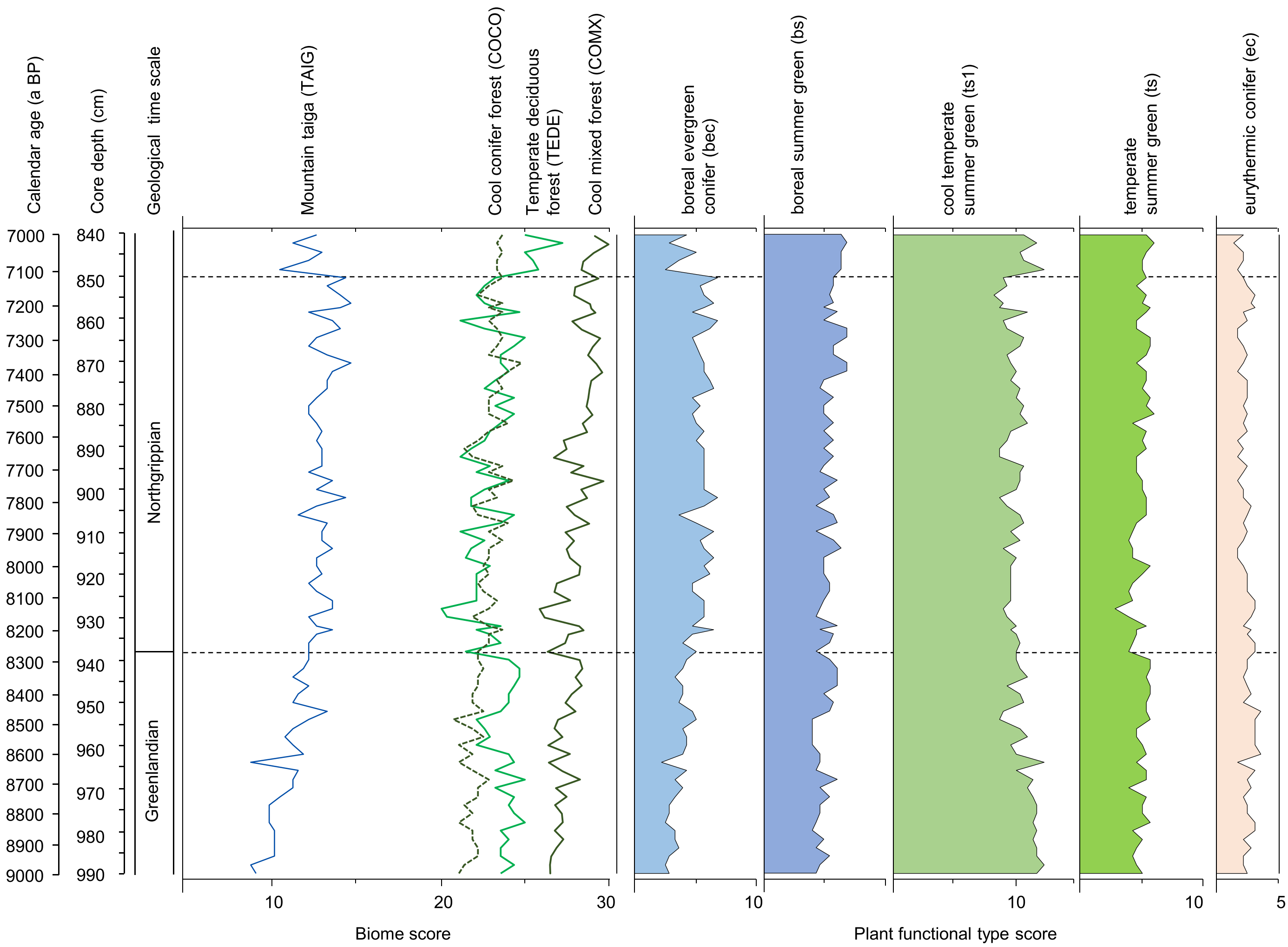

Fig. 5. Main results of the plant functional type (PFT) score calculation and pollen-based biome reconstruction obtained for the analysed section of sediment core MO-05 from Lake Mondsee on depth and age scale (this study).

that spruce trees in Austrian forests can be particularly affected by frequent droughts, storms and wildfires. For example, Norway spruce (*Picea abies* (L.) Karst.) has suffered from the disastrous storms of 2007 and 2008, which left gaps and shrub areas on former coniferous stands with an area of 95,000 ha (Russ, 2011). In the absence of a noticeable increase in the concentrations of microcharcoal particles in the MO-05 sediments (Fig. 6f), storm damage might explain the decrease in *Picea* pollen at about 7100 a BP. The short-term peak of *Corylus* pollen shortly after 7100 a BP could be the result of increasing anthropogenic pressure on forest vegetation (e.g. Rey et al., 2019; Rösch et al., 2021), but the absence of other indicators of human activity does not further support such an interpretation.

5.2. Reflection of the 8.2 ka BP event in the Lake Mondsee proxy records

The 8.2 ka BP event and its manifestation in environmental archives around the world is a hot topic of Holocene palaeogeographic and palaeoclimatic research aiming at a better understanding of the triggers and spatio-temporal responses of environmental systems (and their physical, biological and social components) to rapid climate changes. It is well-recognised in $\delta^{18}O$ records from Greenland ice cores (e.g. Fig. 6i; Svensson et al., 2008), which are frequently used as an indicator of Northern Hemisphere temperature changes, as well as in global speleothem records (e.g. Parker and Harrison, 2022). However, in other well-dated climate records, representing both larger (e.g. Fig. 6h) and smaller regions (e.g. Fig. 6g), the 8.2 ka BP event is often not clearly expressed, which complicates interregional correlations and interpretations of its impact and questions the sensitivity of various archives and proxies. Moreover, urging to identify the event in geological archives can substantially bias the interpretation of newly obtained proxy records, particularly for those without a very robust age control, as demonstrated by an objective statistical analysis of abrupt changes around 8.2 ka BP in the Asian summer monsoon domain (Morrill et al., 2003).

A sub-decadal $\delta^{18}O$ record obtained from the calcareous valves of benthic ostracods preserved in the MO-05 sediments (Fig. 6j) reveals a clear reflection of the 8.2 ka BP event that is in agreement with other stable isotope records from the North Atlantic region with respect to the timing, duration and magnitude of the event (Andersen et al., 2017). Based on this record, the mean annual air temperature at Lake Mondsee during the 8.2 ka BP event decreased by ~1.5 °C relative to the pre-event level (Andersen et al., 2017). This is similar to the temperature drop seen in the ostracod $\delta^{18}O$-based mean annual air temperature reconstruction from Lake Ammersee (von Grafenstein et al., 1998), located ~170 km west of Lake

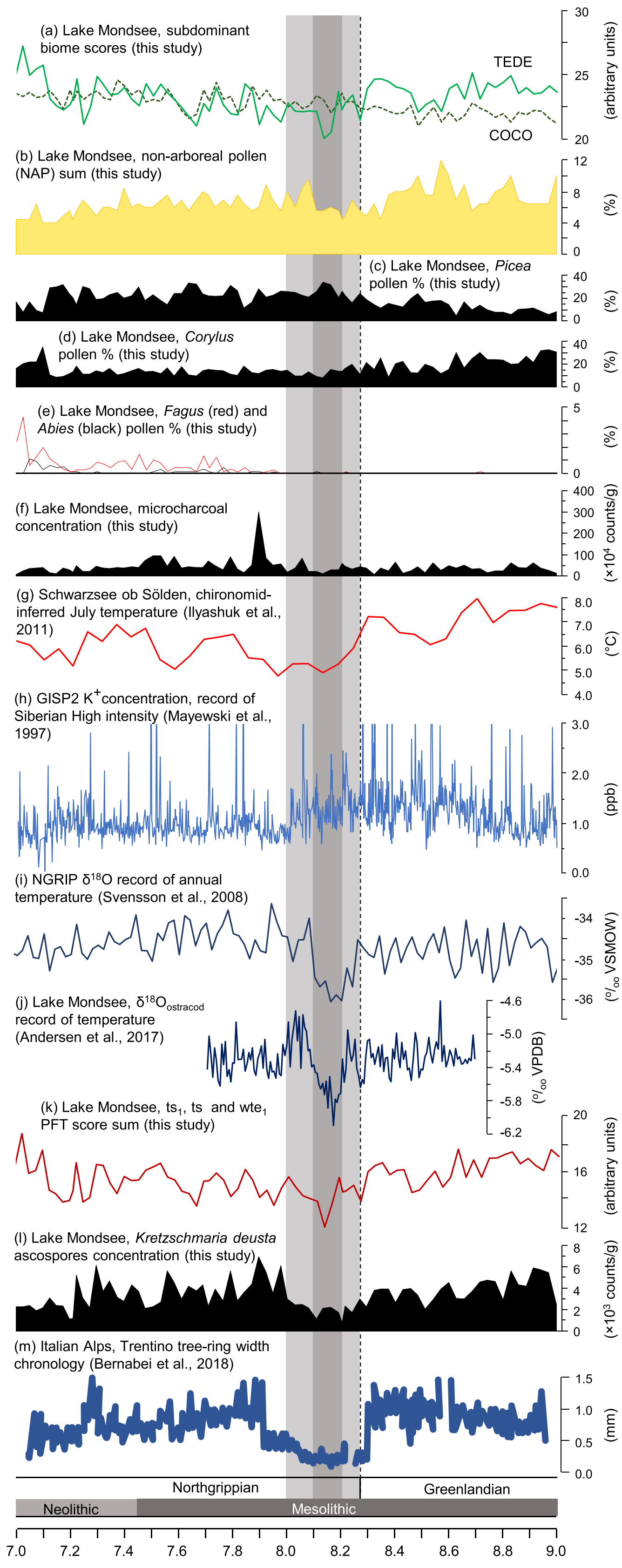

Fig. 6. Selected results of this study along with published proxy records discussed in the text. (a) Changes in the numerical scores of the temperate deciduous (TEDE) and cool conifer (COCO) forest biomes in the Lake Mondsee catchment; (b) changes in the percentages of non-arboreal pollen (NAP) taxa in the MO-05 record; changes in the percentages of some characteristic pollen taxa discussed in the text: (c) *Picea*, (d) *Corylus*, (e) *Fagus* and *Abies*; (f) microcharcoal concentration in the MO-05 record; (g) mean July temperature inferred from the chironomid record from Lake Schwarzsee ob Sölden, Austria (Ilyashuk et al., 2011); (h) GISP2 K^+ concentration record of Siberian High intensity (Mayewski et al., 1997); (i) NGRIP $\delta^{18}O$ record of annual temperature (Svensson et al., 2008); (j) $\delta^{18}O_{ostracod}$ record of temperature from sediment core MO-05 from Lake Mondsee (Andersen et al., 2017); (k) sum of the cold-intolerant PFT scores (i.e. ts_1, ts and wte_1) in the MO-05 record (this study); (l) changes in the *Kretzschmaria deusta* ascospores concentration in the MO-05 record from Lake Mondsee (this study); (m) annual changes in tree-ring width (mm) derived from the Trentino chronology, Italian Alps (adapted from Bernabei et al., 2018). The vertical black dashed line shows the Greenlandian–Northgrippian boundary at 8276 a BP. The vertical light grey bar indicates the interval between 8280 and 8000 a BP, which is commonly associated with the 8.2 ka BP event, and the dark grey bar highlights the interval of most pronounced cooling ca. 8200–8100 a BP.

Mondsee, and also fits estimates from other European palaeoclimate proxy records (e.g. Feurdean et al., 2008; Morrill et al., 2013; Veski et al., 2004).

At first glance, the bi-decadal pollen record from Lake Mondsee (Fig. 3) provides no direct reflection of the 8.2 ka BP event but reveals a rather protracted shift from *Corylus*-dominated to *Picea*-dominated pollen assemblages, marking the boundary between the Early and Middle Holocene, i.e. the Greenlandian and the Northgrippian, at about 8280–8270 a BP. Indeed, without the very robust chronology that is available for sediment core MO-05, any of the frequent small-scale fluctuations in the pollen curves could be regarded as the 8.2 ka BP event. Alternatively, one could conclude that the vegetation of the Lake Mondsee region was ‘insensitive’ to the most severe Holocene cooling event in the Northern Hemisphere.

Indeed, Lauterbach et al. (2011) demonstrated that even a much stronger cooling like the Younger Dryas, about 12,700–11,600 years ago, only left a relatively subtle imprint in the pollen percentage/concentration record from Lake Mondsee compared to sites at higher altitudes or closer to the remnants of the Scandinavian Ice Sheet (e.g. in the Eifel region; Litt and Stebich, 1999). Considering that European pollen records at higher latitudes partly show a more distinct vegetation response to the 8.2 ka BP event even in individual taxa (e.g. Veski et al., 2004), site characteristics certainly play a major role for detecting the event in the pollen data. Furthermore, Seppä et al. (2007) suggested that the 8.2 ka BP event was more a winter cooling and that there has been a distinct regional zonation in its reflection, i.e. in terms of “latitudinal belts” with variable event strength. Our current study highlights that the 8.2 ka BP event is not always visible by conventional (i.e. visual) interpretation of pollen diagrams from southern Central Europe (e.g. Dietre et al., 2014; Litt et al., 2009; Rey et al., 2013) and emphasises the objective quantitative biomization as a suitable approach to overcome this problem.

In order to use vegetation models and fossil pollen records as a diagnostic tool for palaeoclimate simulations, Prentice et al. (1996) proposed a method for the objective ‘biomization’ of pollen data based on fuzzy logic and taking into account the growing conditions and bioclimatic tolerance of pollen-producing plants. The pollen-based biome reconstruction applied to the MO-05 pollen record (Fig. 5) reveals on the one hand a major change in regional vegetation after ca. 8280 a BP, but shows on the other hand also a major drop in the TEDE biome scores, culminating around 8165–8135 a BP (Fig. 6a). A similar result is demonstrated by the sum of PFTs (Fig. 6k), including warm-loving broadleaved tree and shrub taxa (Prentice et al., 1996, Table 2), which suggests that the reaction of the local forests to the cooling culminated around 8140 a BP, i.e. synchronously (within the dating uncertainty) with the July temperature minimum (superimposed on the general temperature decrease) derived from the chironomid record of Lake

Schwarzsee ob Sölden (Fig. 6g; Ilyashuk et al., 2011) and the minimum in the NGRIP δ^{18}O record from Greenland (Fig. 6i; Svensson et al., 2008). The comparison with the ostracod δ^{18}O record from Lake Mondsee (Fig. 6j; Andersen et al., 2017), which has been obtained from the same sediment core and uses the same chronology, reveals, however, a delay of ca. 30–35 years for the vegetation response, possibly indicating a "response lag" of the local vegetation to the climatic forcing in the order of a few decades.

The NPP taxa in the MO-05 record (Fig. 4) are inconclusive with respect to the 8.2 ka BP cooling. For example, the green algae *Botryococcus* shows a clear change in the concentration curve towards higher (albeit fluctuating) values after ca. 8280 a BP, which indicates a stepwise change in the regional climate regime at the Greenlandian–Northgrippian boundary, rather than a single cold event. On the contrary, a notable minimum concentration of *K. deusta* ascospores centred at 8220–8100 a BP (Fig. 6l) falls well within the 8.2 ka BP event. *K. deusta* is a parasitic fungus and plant pathogen common on a wide range of broadleaved trees including beech, oak, lime and maple (van Geel et al., 2013). New fruiting bodies are formed in spring and thus could be affected by late frost. The effect of temperature on mycelial growth of *K. deusta* was experimentally studied by Cordin et al. (2021), who showed that optimum growth occurred at 25 °C, whereas growth was reduced at 10 °C. This finding is in general agreement with field observations from the region of Trentino (Dolomitic Alps, between 780 and 1630 m a.s.l.), suggesting a link between the observed increased spread of *K. deusta* and the recent rise in average annual temperatures and the number of days with a mean temperature above 18 °C in the region (Cordin et al., 2021). Reconstructions of Holocene forest dynamics in the United Kingdom (Innes et al., 2006) and Poland (Latałowa et al., 2013) also suggested *K. deusta* as a proxy for the Middle Holocene climate and hypothesized an increased risk of *K. deusta* outbreaks under climate warming. Our data (Fig. 6l) reveal a sensitive response of this species to the cooling during the 8.2 ka BP event as well as to the subsequent warming reflected by the ostracod δ^{18}O record (Andersen et al., 2017), eventually indicating the potential of *K. deusta* to track past temperature variations. The record of changes in ring width from the very accurate Trentino chronology (Fig. 6m) based on Holocene tree remains from temperature-controlled high-elevation sites in the Italian part of the Eastern Alps (Bernabei et al., 2018, Fig. 1b) supports this conclusion as it shows a very good agreement with the *K. deusta* record (Fig. 6l) and the pollen-based vegetation reconstruction (Fig. 6a, k) from Lake Mondsee. Van Geel et al. (2013) interpreted ascospores of *K. deusta* in event layers in the sediments of Lake Meerfelder Maar in Germany as rainstorm indicators during a Late Holocene beech-forest phase. However, this relationship cannot be confirmed for the MO-05 sediments as microfacies and geochemical analyses revealed no significant changes in sediment composition and particularly no increase in the number of flood event layers across the interval encompassing the isotopically defined 8.2 ka BP event (Andersen et al., 2017), indicating the absence of significant changes in precipitation-driven input of detrital material to the lake.

6. Conclusions

The 8.2 ka BP event represents the most prominent climate event during the Holocene and has therefore been used to formally define the boundary between the Early and Middle Holocene, i.e. the Greenlandian and the Northgrippian. However, persistent climate and/or ecosystem shifts except the short-term climate perturbation at 8.2 ka BP have not been documented so far for this boundary, leaving it rather formal and arbitrary. In the present study we show that high-resolution pollen data from the varve-dated sediment core MO-05 from Lake Mondsee, Austria, are suitable to identify both the vegetation impact of the short-term cooling at 8.2 ka BP as well as a synchronous sustained shift in local biomes at the Greenlandian–Northgrippian boundary. In the vegetation composition, the transition between the Greenlandian and the Northgrippian is marked by the progressive expansion of *Picea* and the parallel decline of *Corylus*. However, the Greenlandian–Northgrippian boundary itself is not clearly visible in individual taxa pollen curves, concentrations and the AP/NAP ratio. In contrast, applying the objective biomization method to the fossil pollen data shows a well-defined shift in the TEDE and COCO biome scores, which reflects a decreasing role of temperate broadleaved trees and shrubs and a strengthening of boreal conifers in the study area at ca. 8280 a BP, synchronous to the currently proposed Greenlandian–Northgrippian boundary. The same applies to the 8.2 ka BP event. While this cold phase is not clearly visible in the proportions of individual pollen taxa, it can be pinpointed by a pronounced decline in the temperate deciduous biome scores and in the summed scores of warm-loving tree and shrub taxa at 8165–8135 a BP. The obtained results together with the published δ^{18}O record of benthic ostracods and the newly generated *K. deusta* record from sediment core MO-05 confirm the climatic sensitivity of these proxies and the high potential of the Lake Mondsee sediment archive for reconstructing Holocene environmental variability in southern Central Europe. Our study also demonstrates the suitability of the biomization method for identifying climate transitions and short-term climate fluctuations, which are sometimes overlooked by the conventional examination of individual pollen taxa curves.

Author contribution

AS and PET conceptualised the study and devised the methodology. SL provided the age-depth model. AS, SL and PET performed sediment sampling, while AS completed laboratory processing and palynological analysis, generated the results, and prepared the diagrams and the initial text. AB and PET acquired the funding. CL drafted the maps in Fig. 1, while SL and PET compiled Fig. 2. All co-authors discussed the results and contributed to the writing and editing of the final manuscript.

Funding

Lake coring was carried out within the European Science Foundation EuroCLIMATE project DecLakes (04-ECLIM-FP29). A. Brauer acknowledges funding by the DFG (Deutsche Forschungsgemeinschaft) through project BR 2208/2-2. This work is part of the PhD project of A. Schubert, contributing to the project "Individual life histories in long-term culture change: Holocene hunter-gatherers in Northern Eurasia", financed by the Social Sciences and Humanities Research Council of Canada (SSHRC Partnership Grant No. 895-2018-1004), and the 'Bridging Eurasia' Research Initiative, supported by the DFG (TA 540/4-1, TA 540/8-1), the FU Berlin and the German Archaeological Institute (DAI).

Declaration of competing interest

The authors declare that they have no known competing financial interests or personal relationships that could have appeared to influence the work reported in this paper.

Data availability

We provided original data in the Supplementary Data

Acknowledgements

Anna Schubert would like to thank Aleksandra Krikunova for drafting Fig. 6l, Dr. Franziska Kobe and Maike Glos (all FU Berlin) for their support in laboratory work, and Dr. Susanne Jahns (Brandenburgisches Landesamt für Denkmalpflege und Archäologisches Landesmuseum, Wünsdorf) and Dr. Magdalena Wieckowska-Lüth (Institute of Prehistoric and Protohistoric Archaeology, Kiel University) for helpful consultations. We extend our gratitude to the handling editor Prof. Dr. Donatella Magri and two anonymous reviewers, whose careful reading and valuable comments helped to improve this paper.

Appendix A. Supplementary data

Supplementary data related to this article can be found at https://doi.org/10.1016/j.quascirev.2023.108073.

References

Alley, R.B., Mayewski, P.A., Sowers, T., Stuiver, M., Taylor, K.C., Clark, P.U., 1997. Holocene climatic instability: a prominent, widespread event 8200 yr ago. Geology 25, 483–486.

Andersen, N., Lauterbach, S., Erlenkeuser, H., Danielopol, D.L., Namiotko, T., Hüls, M., Belmecheri, S., Dulski, P., Nantke, C., Meyer, H., Chapligin, B., von Grafenstein, U., Brauer, A., 2017. Evidence for higher-than-average air temperatures after the 8.2 ka event provided by a Central European δ18O record. Quat. Sci. Rev. 172, 96–108.

Behre, K.-E., 2007. Evidence for mesolithic agriculture in and around central Europe? Veg. Hist. Archaeobotany 16, 203–219.

Beiwl, C., Mühlemann, H., 2008. Atlas der natürlichen Seen Österreichs mit einer Fläche ≥50 ha. Morphometrie–Typisierung–Trophie. Bundesamt für Wasserwirtschaft, Vienna.

Bennett, K.D., Willis, K.J., 2001. Pollen. In: Smol, J.P., Birks, J.H.B., Last, W.M., Bradley, R.S., Alverson, K. (Eds.), Tracking Environmental Change Using Lake Sediments. Volume 3: Terrestrial, Algal and Siliceous Indicators. Kluwer, Dordrecht, pp. 5–32.

Berglund, B.E., Ralska-Jasiewiczowa, M., 1986. Pollen analysis and pollen diagrams. In: Berglund, B.E. (Ed.), Handbook of Holocene Palaeoecology and Palaeohydrology. Wiley Interscience, New York, pp. 455–484.

Bernabei, M., Bontadi, J., Nicolussi, K., 2018. Observations on Holocene subfossil tree remains from high-elevation sites in the Italian Alps. Holocene 28, 2017–2027.

Beug, H.-J., 2004. Leitfaden der Pollenbestimmung: für Mitteleuropa und angrenzende Gebiete. Pfeil, München.

Brauer, A., Hajdas, I., Blockley, S.P.E., Bronk Ramsey, C., Christl, M., Ivy-Ochs, S., Moseley, G.E., Nowaczyk, N.N., Rasmussen, S.O., Roberts, H.M., Spötl, C., Staff, R.A., Svensson, A., 2014. The importance of independent chronology in integrating records of past climate change for the 60-8 ka INTIMATE time interval. Quat. Sci. Rev. 106, 47–66.

Bronk Ramsey, C., 1995. Radiocarbon calibration and analysis of stratigraphy: the OxCal program. Radiocarbon 37, 425–430.

Bronk Ramsey, C., Staff, R.A., Bryant, C.L., Brock, F., Kitagawa, H., van der Plicht, J., Schlolaut, G., Marshall, M.H., Brauer, A., Lamb, H.F., Payne, R.L., Tarasov, P.E., Haraguchi, T., Gotanda, K., Yonenobu, H., Yokoyama, Y., Tada, R., Nakagawa, T., 2012. A complete terrestrial radiocarbon record for 11.2 to 52.8 kyr B.P. Science 338, 370–374.

Clark, J.S., 1988. Particle motion and theory of charcoal analysis: source area, transport, deposition, and sampling. Quat. Res. 30, 67–80.

Clark, J.S., Merkt, J., Müller, H., 1989. Post-glacial fire, vegetation, and human history on the northern alpine forelands, south-western Germany. J. Ecol. 77, 897–925.

Cordin, G., Messina, G., Maresi, G., Zottele, F., Ferretti, F., Montecchio, L., Longa, C.M.O., 2021. *Kretzschmaria deusta*, a limiting factor for survival and safety of veteran beech trees in Trentino (Alps, Northern Italy). iForest 14, 576–581.

Davis, B.A., Brewer, S., Stevenson, A.C., Guiot, J., Contributors, Data, 2003. The temperature of Europe during the Holocene reconstructed from pollen data. Quat. Sci. Rev. 22, 1701–1716.

DeFries, R.S., Hansen, M.C., Townshend, J.R.G., 2000. Global continuous fields of vegetation characteristics: a linear mixture model applied to multi-year 8 km AVHRR data. Int. J. Rem. Sens. 21, 1389–1414.

Demske, D., Tarasov, P.E., Nakagawa, T., Suigetsu, 2013. Atlas of pollen, spores and further non-pollen palynomorphs recorded in the glacial-interglacial late Quaternary sediments of Lake Suigetsu, central Japan, 2006 Project Members Quat. Int. 164–238, 290–291.

Dietre, B., Walser, C., Lambers, K., Reitmaier, T., Hajdas, I., Haas, J.N., 2014. Palaeoecological evidence for Mesolithic to Medieval climatic change and anthropogenic impact on the Alpine flora and vegetation of the Silvretta Massif (Switzerland/Austria). Quat. Int. 353, 3–16.

Dimbleby, G.W., 1985. The Palynology of Archaeological Sites. Academic Press, New York.

Draxler, I., 1977. Pollenanalytische Untersuchungen von Mooren zur spät- und postglazialen Vegetationsgeschichte im Einzugsgebiet der Traun. Jahrbuch der Geologischen Bundesanstalt 120, 131–163.

Duan, P., Li, H., Sinha, A., Voarintsoa, N.R.G., Kathayat, G., Hu, P., Zhang, H., Ning, Y., Cheng, H., 2021. The timing and structure of the 8.2 ka event revealed through high-resolution speleothem records from northwestern Madagascar. Quat. Sci. Rev. 268, 107104.

Fægri, K., Iversen, J., 1989. Textbook of Pollen Analysis. John Wiley & Sons, Chichester.

Feurdean, A., Klotz, S., Mosbrugger, V., Wohlfarth, B., 2008. Pollen-based quantitative reconstructions of Holocene climate variability in NW Romania. Palaeogeogr. Palaeoclimatol. Palaeoecol. 260, 494–504.

Finsinger, W., Tinner, W., 2007. Pollen and plant macrofossils at Lac de Fully (2135 m a.s.l.): Holocene forest dynamics on a highland plateau in the Valais, Switzerland. Holocene 17, 1119–1127.

Flohr, P., Fleitmann, D., Matthews, R., Matthews, W., Black, S., 2016. Evidence of resilience to past climate change in Southwest Asia: early farming communities and the 9.2 and 8.2 ka events. Quat. Sci. Rev. 136, 23–39.

Fuchs, K., Hacker, W., Pinterits, S., 2004. Raumeinheit Attersee-Mondsee-Becken. Natur und Landschaft/Leitbilder für Oberösterreich. Bandwagon 12, 1–91.

Fuchs, K., Hacker, W., Nußbaumer, E., 2005. Naturraumkartierung Oberösterreich. Landschaftserhebung Gemeinde Innerschwand. Endbericht. Gutachten Naturschutzabteilung Oberösterreich 1–64, 0386.

García-Escárzaga, A., Gutiérrez-Zugasti, I., Marín-Arroyo, A.B., Fernandes, R., Núñez de la Fuente, S., Cuenca-Solana, D., Iriarte, E., Simões, C., Martín-Chivelet, J., González-Morales, M.R., Roberts, P., 2022. Human forager response to abrupt climate change at 8.2 ka on the Atlantic coast of Europe. Sci. Rep. 12, 6481.

Geiger, R., 1954. Klassifikation der Klimate nach W. Köppen. Landolt-Börnstein – Zahlenwerte und Funktionen aus Physik, Chemie, Astronomie, Geophysik und Technik, alte Serie 3. Springer, Berlin, pp. 603–607.

Giesecke, T., Hickler, T., Kunkel, T., Sykes, M.T., Bradshaw, R.H.W., 2007. Towards an understanding of the Holocene distribution of *Fagus sylvatica* L. J. Biogeogr. 34, 118–131.

González-Sampériz, P., Utrilla, P., Mazo, C., Valero-Garcés, B., Sopena, M.C., Morellón, M., Sebastián, M., Moreno, A., Martínez-Bea, M., 2009. Patterns of human occupation during the early Holocene in the Central Ebro Basin (NE Spain) in response to the 8.2 ka climatic event. Quat. Res. 71, 121–132.

Griffiths, S., Robinson, E., 2018. The 8.2 ka BP Holocene climate change event and human population resilience in northwest Atlantic Europe. Quat. Int. 465, 251–257.

Grimm, E.C., 1993. TILIA 2.0 Version b.4 (Computer Software). Illinois State Museum. Research and Collections Center, Springfield.

Grimm, E.C., 2004. TGView. Illinois State Museum. Research and Collections Center, Springfield.

Ilyashuk, E.A., Koinig, K.A., Heiri, O., Ilyashuk, B.P., Psenner, R., 2011. Holocene temperature variations at a high-altitude site in the Eastern Alps: a chironomid record from Schwarzsee ob Sölden, Austria. Quat. Sci. Rev. 30, 176–191.

Innes, J., Blackford, J., Chambers, F., 2006. *Kretzschmaria deusta* and the northwest European Mid-Holocene *Ulmus* decline at Moel Y Gerddi, North Wales, United Kingdom. Palynology 30, 121–132.

Irlweck, K., Danielopol, D.L., 1985. Caesium-137 and lead-210 dating of recent sediments from Mondsee (Austria). Hydrobiologia 128, 175–185.

Jarvis, A., Reuter, H.I., Nelson, A., Guevara, E., 2008. Hole-filled Seamless SRTM Data V4. International Centre for Tropical Agriculture (CIAT).

Kämpf, L., Brauer, A., Swierczynski, T., Czymzik, M., Müller, P., Dulski, P., 2014. Deciphering processes of flood-triggered detrital layer deposition in the Lake Mondsee sediment record using a dual calibration approach. J. Quat. Res. 29, 475–486.

Kämpf, L., Mueller, P., Plessen, B., Naumann, R., Thoss, H., Güntner, A., Merz, B., Brauer, A., 2015. Hydrological and sedimentological processes of flood layer formation in Lake Mondsee. Depositional Record 1, 18–37.

Kämpf, L., Plessen, B., Lauterbach, S., Nantke, C., Meyer, H., Chapligin, B., Brauer, A., 2020. Stable oxygen and carbon isotopes of carbonates in lake sediments as a paleoflood proxy. Geology 48, 3–7.

Kern, A., Kowarik, K., Reschreiter, H., Rausch, A.W., Thommes, J., Taylor, T.G., 2009. Kingdom of Salt: 7000 years of Hallstatt. Naturhistorisches Museum Wien, Vienna.

Kleinen, T., Tarasov, P., Brovkin, V., Andreev, A., Stebich, M., 2011. Comparison of modeled and reconstructed changes in forest cover through the past 8000 years: Eurasian perspective. Holocene 21, 723–734.

Kleinmann, A., Merkt, J., Müller, H., 2015. Sedimente des Degersees: ein Umweltarchiv – Sedimentologie und Palynologie. In: Mainberger, M., Merkt, J., Kleinmann, A. (Eds.), Pfahlbausiedlungen am Degersee – Archäologische und naturwissenschaftliche Untersuchungen. Theiss, Darmstadt, pp. 409–471.

Kobashi, T., Severinghaus, J.P., Brook, E.J., Barnola, J.-M., Grachev, A.M., 2007. Precise timing and characterization of abrupt climate change 8200 years ago from air trapped in polar ice. Quat. Sci. Rev. 26, 1212–1222.

Kobe, F., Bezrukova, E.V., Leipe, C., Shchetnikov, A.A., Goslar, T., Wagner, M., Kostrova, S.S., Tarasov, P.E., 2020. Holocene vegetation and climate history in Baikal Siberia reconstructed from pollen records and its implications for archaeology. Archaeological Research in Asia 23, 100209.

Kobe, F., Hoelzmann, P., Gliwa, J., Olschewski, P., Peskov, S.A., Shchetnikov, A.A., Danukalova, G.A., Osipova, E.M., Goslar, T., Leipe, C., Wagner, M., Bezrukova, E.V., Tarasov, P.E., 2022. Lateglacial–Holocene environments and human occupation

in the Upper Lena region of Eastern Siberia derived from sedimentary and zooarchaeological data from Lake Ochaul. Quat. Int. 623, 139–158.
Kohl, H., 1998. Das Eiszeitalter in Oberösterreich Teil II: Die Eiszeitliche Vergletscherung in Oberösterreich. Jahrbuch des Oberösterreichischen Musealvereins, Linz, pp. 175–390.
Krikunova, A.I., Kostromina, N.A., Savelieva, L.A., Tolstobrov, D.S., Petrov, A.Y., Long, T., Kobe, F., Leipe, C., Tarasov, P.E., 2022. Late- and postglacial vegetation and climate history of the central Kola Peninsula derived from a radiocarbon-dated pollen record of Lake Kamenistoe. Palaeogeogr. Palaeoclimatol. Palaeoecol. 603, 111191.
Köppen, W.P., 1923. Die Klimate der Erde: Grundriss der Klimakunde. Walter de Gruyter, Berlin.
Kunze, W., 1986. Mondsee – 5000 Jahre Geschichte und Kultur. Selbstverlag der Gemeinde, Mondsee.
Kutzbach, J.E., Webb III, T., 1993. Conceptual basis for understanding Late Quaternary climates. In: Wright, Jr., H.E., Kutzbach, J.E., Webb III, T., Ruddiman, W.F., Street-Perrott, F.A., Bartlein, P.J. (Eds.), Global Climates since the Last Glacial Maximum. University of Minnesota Press, Minneapolis, pp. 5–11.
Laskar, J., Robutel, P., Joutel, F., Gastineau, M., Correia, A.C.M., Levrard, B., 2004. A long-term numerical solution for the insolation quantities of the earth. Astron. Astrophys. 428, 261–285.
Latałowa, M., Pędziszewska, A., Maciejewska, E., Święta-Musznicka, J., 2013. *Tilia* forest dynamics, *Kretzschmaria deusta* attack, and mire hydrology as palaeoecological proxies for mid-Holocene climate reconstruction in the Kashubian Lake District (N Poland). Holocene 23, 667–677.
Lauterbach, S., Brauer, A., Andersen, N., Danielopol, D.L., Dulski, P., Hüls, M., Milecka, K., Namiotko, T., Obremska, M., von Grafenstein, U., Participants, Declakes, 2011. Environmental responses to Lateglacial climatic fluctuations recorded in the sediments of pre-Alpine Lake Mondsee (northeastern Alps). J. Quat. Sci. 26, 253–267.
Lechterbeck, J., Rösch, M., 2021. Böhringer See, western Lake Constance (Germany): an 8500 year record of vegetation change. Grana 60, 119–131.
Leipe, C., Kobe, F., Müller, S., 2019. Testing the performance of sodium polytungstate and lithium heteropolytungstate as non-toxic dense media for pollen extraction from lake and peat sediment samples. Quat. Int. 516, 207–214.
Li, H., Renssen, H., Roche, D.M., Miller, P.A., 2019. Modelling the vegetation response to the 8.2 ka bp cooling event in Europe and Northern Africa. J. Quat. Sci. 34, 650–661.
Litt, T., Stebich, M., 1999. Bio- and chronostratigraphy of the lateglacial in the Eifel region, Germany. Quat. Int. 61, 5–16.
Litt, T., Schölzel, C., Kühl, N., Brauer, A., 2009. Vegetation and climate history in the Westeifel Volcanic Field (Germany) during the past 11000 years based on annually laminated lacustrine maar sediments. Boreas 38, 679–690.
Magny, M., 2004. Holocene climate variability as reflected by mid-European lake-level fluctuations and its probable impact on prehistoric human settlements. Quat. Int. 113, 65–79.
Magny, M., Begeot, C., Guiot, J., Peyron, O., 2003. Contrasting patterns of hydrological changes in Europe in response to Holocene climate cooling phases. Quat. Sci. Rev. 22, 1589–1596.
Magri, D., Vendramin, G.G., Comps, B., Dupanloup, I., Geburek, T., Gömöry, D., Latałowa, M., Litt, T., Paule, L., Roure, J.M., Tantau, I., Van Der Knaap, W.O., Petit, R.J., de Beaulieu, J.-L., 2006. A new scenario for the Quaternary history of European beech populations: palaeobotanical evidence and genetic consequences. New Phytol. 171, 199–221.
Margold, M., Stokes, C.R., Clark, C.D., 2018. Reconciling records of ice streaming and ice margin retreat to produce a palaeogeographic reconstruction of the deglaciation of the Laurentide Ice Sheet. Quat. Sci. Rev. 189, 1–30.
Martin-Puertas, C., Walsh, A.A., Blockley, S.P.E., Harding, P., Biddulph, G.E., Palmer, A., Ramisch, A., Brauer, A., 2021. The first Holocene varve chronology for the UK: based on the integration of varve counting, radiocarbon dating and tephrostratigraphy from Diss Mere (UK). Quat. Geochronol. 61, 101134.
Mayewski, P., Meeker, L.D., Twickler, M.S., Whitlow, S., Yang, Q., Prentice, M., 1997. Major features and forcing of high latitude northern hemisphere circulation using a 110,000-year-long glaciochemical series. J. Geophys. Res. 102, 26345–26366.
Mayewski, P.A., Rohling, E.E., Stager, J.C., Karlén, W., Maasch, K.A., Meeker, L.D., Meyerson, E.A., Gasse, F., van Kreveld, S., Holmgren, K., Lee-Thorp, J., Rosqvist, G., Rack, F., Staubwasser, M., Schneider, R.R., Steig, E.J., 2004. Holocene climate variability. Quat. Res. 62, 243–255.
Moore, P.D., Webb, J.A., 1978. An Illustrated Guide to Pollen Analysis. Hodder and Stoughton (London-Sydney-Auckland-Toronto).
Morrill, C., Overpeck, J.T., Cole, J.E., 2003. A synthesis of abrupt changes in the Asian summer monsoon since the last deglaciation. Holocene 13, 465–476.
Morrill, C., Anderson, D.M., Bauer, B.A., Buckner, R., Gille, E.P., Gross, W.S., Hartman, M., Shah, A., 2013. Proxy benchmarks for intercomparison of 8.2 ka simulations. Clim. Past 9, 423–432.
Morrill, C., Ward, E.M., Wagner, A.J., Otto-Bliesner, B.L., Rosenbloom, N., 2014. Large sensitivity to freshwater forcing location in 8.2 ka simulations. Paleoceanography 29, 930–945.
Nakagawa, T., Gotanda, K., Haraguchi, T., Danhara, T., Yonenobu, H., Yokoyama, Y., Brauer, A., Yokoyama, Y., Tada, R., Takemura, K., Staff, R.A., Payne, R., Bronk Ramsey, C., Bryant, C., Brock, F., Schlolaut, G., Marshall, M., Tarasov, P., Lamb, H., Suigetsu 2006 Project Members, 2012. SG06, a perfectly continuous and varved sediment core from Lake Suigetsu, Japan: stratigraphy and potential for improving the radiocarbon calibration model and understanding of late Quaternary climate changes. Quat. Sci. Rev. 36, 164–176.
Nakagawa, T., Tarasov, P., Staff, R., Bronk Ramsey, C., Marshall, M., Schlolaut, G., Bryant, C., Brauer, A., Lamb, H., Haraguchi, T., Gotanda, K., Kitaba, I., Kitagawa, H., van der Plicht, J., Yonenobu, H., Omori, T., Yokoyama, Y., Tada, R., Yasuda, Y., Suigetsu 2006 Project Members, 2021. The spatio-temporal structure of the Lateglacial to early Holocene transition reconstructed from the pollen record of Lake Suigetsu and its precise correlation with other key global archives: implications for palaeoclimatology and archaeology. Global Planet. Change 202, 103493.
Namiotko, T., Danielopol, D.L., von Grafenstein, U., Lauterbach, S., Brauer, A., Andersen, N., Hüls, M., Milecka, K., Baltanás, A., Geiger, W., DecLakes Participants, 2015. Palaeoecology of Late Glacial and Holocene profundal Ostracoda of pre-Alpine lake Mondsee (Austria) - a base for further (palaeo-) biological research. Palaeogeograp., Paleoclimatol., Paleoecol. 419, 23–36.
Nationalpark O.ö. Kalkalpen GmbH, 2016. Natürliche Buchenwälder des Nationalpark Kalkalpen, Schutz und Erbe alter Wälder, Schriftenreihe Nationalpark Kalkalpen Band 16.
Offenberger, J., 2012. Weltkulturerbe "See" – Ein Forschungsbericht. Mondseer Dokumentationen, Mondseer Museen, Mondsee, p. 96.
Parker, S.E., Harrison, S.P., 2022. The timing, duration and magnitude of the 8.2 ka event in global speleothem records. Sci. Rep. 12, 10542.
Peyron, O., Guiot, J., Cheddadi, R., Tarasov, P.E., Reille, M., Beaulieu, J.-L. de, Bottema, S., Andrieu, V., 1998. Climatic reconstruction in Europe from pollen data, 18,000 years before present. Quat. Res. 49, 183–196.
Prentice, I.C., Cramer, W., Harrison, S.P., Leemans, R., Monserud, R.A., Solomon, A.M., 1992. A global biome model based on plant physiology and dominance, soil properties and climate. J. Biogeogr. 19, 117–134.
Prentice, I.C., Guiot, J., Huntley, B., Jolly, D., Cheddadi, R., 1996. Reconstructing biomes from palaeoecological data: a general method and its application to European pollen data at 0 and 6 ka. Clim. Dynam. 12, 185–194.
Pörtner, H.-O., Roberts, D.C., Tignor, M., Poloczanska, E.S., Mintenbeck, K., Alegría, A., Craig, M., Langsdorf, S., Löschke, S., Möller, V., Okem, A., Rama, B. (Eds.), 2022. IPCC, 2022. Climate Change 2022: Impacts, Adaptation, and Vulnerability. Contribution of Working Group II to the Sixth Assessment Report of the Intergovernmental Panel on Climate Change. Cambridge University Press. Cambridge University Press, Cambridge, UK and New York, NY, USA.
Quadt, V., van der Maaten-Theunissen, M., Frank, G., 2013. Integration of Nature Protection in Austrian Forest Policy. INTEGRATE Country Report for Austria. EFICENT-OEF, Freiburg.
Reille, M., 1992. Pollen et spores d'Europe et d'Afrique du nord. Laboratoire de botanique historique et palynologie, URA CNRS, Marseille, France.
Reille, M., 1995. Pollen et spores d'Europe et d'Afrique du nord. Supplement I. Laboratoire de botanique historique et palynologie, URA CNRS, Marseille, France.
Reille, M., 1998. Pollen et spores d'Europe et d'Afrique du nord, Supplement 2. Laboratoire de botanique historique et palynologie, URA CNRS, Marseille, France.
Reimer, P.J., Austin, W.E.N., Bard, E., Bayliss, A., Blackwell, P.G., Bronk Ramsey, C., Butzin, M., Cheng, H., Edwards, R.L., Friedrich, M., Grootes, P.M., Guilderson, T.P., Hajdas, I., Heaton, T.J., Hogg, A.G., Hughen, K.A., Kromer, B., Manning, S.W., Muscheler, R., Palmer, J.G., Pearson, C., van der Plicht, J., Reimer, R.W., Richards, D.A., Scott, E.M., Southon, J.R., Turney, C.S.M., Wacker, L., Adolphi, F., Büntgen, U., Capano, M., Fahrni, S.M., Fogtmann-Schulz, A., Friedrich, R., Köhler, P., Kudsk, S., Miyake, F., Olsen, J., Reinig, F., Sakamoto, M., Sookdeo, A., Talamo, S., 2020. The IntCal20 northern Hemisphere radiocarbon age calibration curve (0–55 cal kBP). Radiocarbon 62, 725–757.
Rey, F., Schwörer, C., Gobet, E., Colombaroli, D., van Leeuwen, J.F., Schleiss, S., Tinner, W., 2013. Climatic and human impacts on mountain vegetation at Lauenensee (Bernese Alps, Switzerland) during the last 14,000 years. Holocene 23, 1415–1427.
Rey, F., Gobet, E., van Leeuwen, J.F.N., Gilli, A., van Raden, U.J., Hafner, A., Wey, O., Rhiner, J., Schmocker, D., Zünd, J., Tinner, W., 2017. Vegetational and agricultural dynamics at Burgäschisee (Swiss Plateau) recorded for 18,700 years by multi-proxy evidence from partly varved sediments. Veg. Hist. Archaeobotany 26, 571–586.
Rey, F., Gobet, E., Schwörer, C., Wey, O., Hafner, A., Tinner, W., 2019. Causes and mechanisms of synchronous succession trajectories in primeval Central European mixed *Fagus sylvatica* forests. J. Ecol. 107, 1392–1408.
Rey, F., Gobet, E., Schwörer, C., Hafner, A., Szidat, S., Tinner, W., 2020. Climate impacts on vegetation and fire dynamics since the last deglaciation at Moossee (Switzerland). Clim. Past 16, 1347–1367.
Rey, F., Brugger, S.O., Gobet, E., Andenmatten, R., Bonini, A., Inniger, H., Maurer, C., Perret-Gentil-dit-Maillard, N., Riederer, J.C., Heiri, O., Tinner, W., Schwörer, C., 2022. 14,500 years of vegetation and land use history in the upper continental montane zone at Lac de Champex (Valais, Switzerland). Veg. Hist. Archaeobotany 31, 377–393.
Rey, F., Mustaphi, C.J.C., Szidat, S., Gobet, E., Heiri, O., Tinner, W., 2023. Radiocarbon sampling efforts for high-precision lake sediment chronologies. Holocene. https://doi.org/10.1177/09596836231151835 (in press).
Rösch, M., Lechterbeck, J., 2016. Seven Millennia of human impact as reflected in a high resolution pollen profile from the profundal sediments of Litzelsee, Lake Constance region, Germany. Veg. Hist. Archaeobotany 25, 339–358.
Rösch, M., Kleinmann, A., Lechterbeck, J., Wick, L., 2014. Botanical off-site and on-site data as indicators of different land use systems: a discussion with examples from Southwest Germany. Veg. Hist. Archaeobotany 23, 121–133.

Rösch, M., Feger, K.-H., Fischer, E., Hinderer, M., Kämpf, L., Kleinmann, A., Lechterbeck, J., Marinova, E., Schwalb, A., Tserendorj, G., Wick, L., 2021. How changes of past vegetation and human impact are documented in lake sediments: paleoenvironmental research in southwestern Germany, a review. In: Rosen, M.R., Finkelstein, D.B., Park Boush, L., Pla-Pueyo, S. (Eds.), Limnogeology: Progress, Challenges and Opportunities. Syntheses in Limnogeology. Springer, Cham, pp. 107–134.
Russ, W., 2011. Mehr Wald für Österreich. In: Waldinventur 2007/2009. BFW Praxis Information, vol. 24, pp. 3–5.
Ruttkay, E., Cichocki, O., Pernicka, E., Pucher, E., 2004. Prehistoric Lacustrine Villages on the Austrian Lakes – Past and Recent Research Developments. Living on the Lake in Prehistoric Europe: 150 Years of Lake-Dwelling Research. Routledge, London, pp. 50–68.
San-Miguel-Ayanz, J., de Rigo, D., Caudullo, G., Houston Durrant, T., Mauri, A. (Eds.), 2016. European Atlas of Forest Tree Species. Publications Office of the European Union, Luxembourg.
Schmidt, R., 1981. Grundzüge der spät- und postglazialen Vegetations- und Klimageschichte des Salzkammergutes (Österreich) aufgrund palynologischer Untersuchungen von See- und Moorprofilen. Mittl. Komm. für Quartärforsch. Österreichischen Akad. Wiss. 3, 1–96.
Schubert, A., Lauterbach, S., Leipe, C., Scholz, V., Brauer, A., Tarasov, P.E., 2020. Anthropogenic and climate controls on vegetation changes between 1500 BCE and 500 CE reconstructed from a high-resolution pollen record from varved sediments of Lake Mondsee, Austria. Palaeogeogr. Palaeoclimatol. Palaeoecol. 559, 109976.
Schulting, R.J., Mannermaa, K., Tarasov, P.E., Higham, T., Bronk Ramsey, C., Khartanovich, V., Moiseyev, V., Gerasimov, D., O'Shea, J., Weber, A., 2022. Radiocarbon dating from Yuzhniy Oleniy Ostrov cemetery reveals complex human responses to socio-ecological stress during the 8.2 ka cooling event. Nat. Ecol. Evolut. 6, 155–162.
Schwörer, C., Colombaroli, D., Kaltenrieder, P., Rey, F., Tinner, W., 2015. Early human impact (5000–3000 BC) affects mountain forest dynamics in the Alps. J. Ecol. 103, 281–295.
Seppä, H., Birks, H.J.B., Giesecke, T., Hammarlund, D., Alenius, T., Antonsson, K., Bjune, A.E., Heikkilä, M., MacDonald, G.M., Ojala, A.E.K., Telford, R.J., Veski, S., 2007. Spatial structure of the 8200 cal yr bp event in Northern Europe. Clim. Past 3, 225–236.
Shumilovskikh, L.S., Tarasov, P., Arz, H.W., Fleitmann, D., Marret, F., Nowaczyk, N., Plessen, B., Schlütz, F., Behling, H., 2012. Vegetation and environmental dynamics in the southern Black Sea region since 18 kyr BP derived from the marine core 22-GC3. Palaeogeogr. Palaeoclimatol. Palaeoecol. 337–338, 177–193.
Stebich, M., Rehfeld, K., Schlütz, F., Tarasov, P.E., Liu, J., Mingram, J., 2015. Holocene vegetation and climate dynamics of NE China based on the pollen record from Sihailongwan Maar Lake. Quat. Sci. Rev. 124, 275–289.
Stockmarr, J., 1971. Tablets with spores used in absolute pollen analysis. Pollen Spores 13, 614–621.
Stroeven, A.P., Hättestrand, C., Kleman, J., Heyman, J., Fabel, D., Fredin, O., Goodfellow, B.W., Harbor, J.M., Jansen, J.D., Olsen, L., Caffee, M.W., Fink, D., Lundqvist, J., Rosqvist, G.C., Strömberg, B., Jansson, K.N., 2016. Deglaciation of Fennoscandia. Quat. Sci. Rev. 147, 91–121.
Svensson, A., Andersen, K.K., Bigler, M., Clausen, H.B., Dahl-Jensen, D., Davies, S.M., Johnsen, S.J., Muscheler, R., Parrenin, F., Rasmussen, S.O., Röthlisberger, R., Seierstad, I., Steffensen, J.P., Vinther, B.M., 2008. A 60000 year Greenland stratigraphic ice core chronology. Clim. Past 4, 47–57.
Swierczynski, T., Brauer, A., Lauterbach, S., Martín-Puertas, C., Dulski, P., von Grafenstein, U., Rohr, C., 2012. A 1600 yr seasonally resolved record of decadal-scale flood variability from the Austrian Pre-Alps. Geology 40, 1047–1050.
Swierczynski, T., Lauterbach, S., Dulski, P., Brauer, A., 2013a. Late Neolithic Mondsee Culture in Austria: living on lakes and living with flood risk? Clim. Past 9, 1601–1612.
Swierczynski, T., Lauterbach, S., Dulski, P., Delgado, J., Merz, B., Brauer, A., 2013b. Mid- to late Holocene flood frequency changes in the northeastern Alps recorded in varved sediments of Lake Mondsee (Upper Austria). Quat. Sci. Rev. 80, 78–90.
Tarasov, P.E., Webb III, T., Andreev, A.A., Afanas'eva, N.B., Berezina, N.A., Bezusko, L.G., Blyakharchuk, T.A., Bolikhovskaya, N.S., Cheddadi, R., Chernavskaya, M.M., Chernova, G.M., Dorofeyuk, N.I., Dirksen, V.G., Elina, G.A., Filimonova, L.V., Glebov, F.Z., Guiot, J., Gunova, V.S., Harrison, S.P., Jolly, D., Khomutova, V.I., Kvavadze, E.V., Osipova, I.M., Panova, N.K., Prentice, I.C., Saarse, L., Sevastyanov, D.V., Volkova, V.S., Zernitskaya, V.P., 1998. Present-day and mid-Holocene biomes reconstructed from pollen and plant macrofossil data from the Former Soviet Union and Mongolia. J. Biogeogr. 25, 1029–1053.
Tarasov, P.E., Bezrukova, E.V., Müller, S., Kostrova, S.S., White, D., 2017. Climate and vegetation history. In: Losey, R.J., Nomokonova, T. (Eds.), Holocene Zooarchaeology of Cis-Baikal. Archaeology in China and East Asia 6 Nünnerich–Asmus. Verlag & Media GmbH, Mainz, pp. 15–26.
Texier, D., de Noblet, N., Harrison, S.P., Haxeltine, A., Jolly, D., Joussaume, S., Laarif, F., Prentice, I.C., Tarasov, P., 1997. Quantifying the role of biosphere-atmosphere feedbacks in climate change: coupled model simulations for 6000 years BP and comparison with palaeodata for northern Eurasia and northern Africa. Clim. Dynam. 13, 865–882.
Tinner, W., Conedera, M., Ammann, B., Gäggeler, H.W., Gedye, S., Jones, R., Sägesser, B., 1998. Pollen and charcoal in lake sediments compared with historically documented forest fires in southern Switzerland since AD 1920. Holocene 8, 31–42.
Tinner, W., Lotter, A.F., 2006. Holocene expansions of *Fagus silvatica* and *Abies alba* in Central Europe: where are we after eight decades of debate? Quat. Sci. Rev. 25, 526–549.
van Geel, B., 1978. A palaeoecological study of Holocene peat bog sections in Germany and The Netherlands, based on the analysis of pollen, spores and macro and microscopic remains of fungi, algae, cormophytes and animals. Rev. Palaeobot. Palynol. 25, 1–120.
van Geel, B., 2001. Non-pollen palynomorphs. In: Smol, J.P., Birks, J.H.B., Last, W.M., Bradley, R.S., Alverson, K. (Eds.), Tracking Environmental Change Using Lake Sediments. Volume 3: Terrestrial, Algal and Siliceous Indicators. Kluwer, Dordrecht, pp. 99–119.
van Geel, B., Engels, S., Martin-Puertas, C., Brauer, 2013. Ascospores of the parasitic fungus *Kretzschmaria deusta* as rainstorm indicators during a late Holocene beech-forest phase around lake Meerfelder Maar, Germany. J. Paleolimnol. 50, 33–40.
van Husen, D., 1979. Verbreitung, Ursachen und Füllung glazial übertiefter Talabschnitte an Beispielen aus den Ostalpen. Eiszeitalt. Ggw. 29, 9–22.
van Husen, D., 1989. The last interglacial-glacial cycle in the eastern Alps. Quat. Int. 3 (4), 115–121.
Vinther, B.M., Clausen, H.B., Johnsen, S.J., Rasmussen, S.O., Andersen, K.K., Buchardt, S.L., Dahl-Jensen, D., Seierstad, I.K., Siggaard-Andersen, M.-L., Steffensen, J.P., Svensson, A.M., Olsen, J., Heinemeier, J., 2006. A synchronized dating of three Greenland ice cores throughout the Holocene. J. Geophys. Res. 111, D13102.
Veski, S., Seppä, H., Ojala, A.E.K., 2004. Cold event at 8200 yr b.p. recorded in annually laminated lake sediments in eastern Europe. Geology 32, 681–684.
von Grafenstein, U., Erlenkeuser, H., Müller, J., Jouzel, J., Johnsen, S., 1998. The cold event 8200 years ago documented in oxygen isotope records of precipitation in Europe and Greenland. Clim. Dynam. 14, 73–81.
von Schnurbein, S. (Ed.), 2009. Atlas der Vorgeschichte. Konrad Theiss Verlag, Stuttgart.
Waelbroeck, C., Labeyrie, L., Michel, E., Duplessy, J.C., McManus, J.F., Lambeck, K., Balbon, E., Labracherie, M., 2002. Sea-level and deep water temperature changes derived from benthic foraminifera isotopic records. Quat. Sci. Rev. 21, 295–305.
Walker, M., Head, M.J., Lowe, J., Berkelhammer, M., Björck, S., Cheng, H., Cwynar, L.C., Fisher, D., Gkinis, V., Long, A., Newnham, R., Rasmussen, S.O., Weiss, H., 2019. Subdividing the Holocene Series/Epoch: formalization of stages/ages and subseries/subepochs, and designation of GSSPs and auxiliary stratotypes. J. Quat. Sci. 34, 173–186.
Weng, C., Hooghiemstra, H., Duivenvoorden, J.F., 2006. Challenges in estimating past plant diversity from fossil pollen data: statistical assessment, problems, and possible solutions. Divers. Distrib. 12, 310–318.
Whitlock, C., Larsen, C.P.S., 2001. Charcoal as a fire proxy. In: Smol, J.P., Birks, J.H.B., Last, W.M., Bradley, R.S., Alverson, K. (Eds.), Tracking Environmental Change Using Lake Sediments. Volume 3: Terrestrial, Algal and Siliceous Indicators. Kluwer, Dordrecht, pp. 75–97.
Wiersma, A.P., Renssen, H., 2006. Model-data comparison for the 8.2 ka BP event: confirmation of a forcing mechanism by catastrophic drainage of Laurentide lakes. Quat. Sci. Rev. 25, 63–88.
Wolf, P., 1977. Die Jagd- und Haustierfauna der spätneolithischen Pfahlbauten des Mondsee. Jahrbuch des Oberösterreichischen Musealvereins 122, 269–347.
Woodward, F.I., 1987. Climate and Plant Distribution. Cambridge University Press, Cambridge, UK.
Yokoyama, Y., Kido, Y., Tada, R., Minami, I., Finkel, R.C., Matsuzaki, H., 2007. Japan Sea oxygen isotope stratigraphy and global sea-level changes for the last 50, 000 years recorded in sediment cores from the Oki Ridge. Palaeogeogr. Palaeoclimatol. Palaeoecol. 247, 5–17.
Zander, P.D., Żarczyński, M., Vogel, H., Tylmann, W., Wacnik, A., Sanchini, A., Grosjean, M., 2021. A high-resolution record of Holocene primary productivity and water-column mixing from the varved sediments of Lake Żabińskie, Poland. Sci. Total Environ. 755, 1–16.
Zagwijn, W.H., 1994. Reconstruction of climate change during the Holocene in western and central Europe based on pollen records of indicator species. Veg. Hist. Archaeobotany 3, 65–88.
Zoller, H., 1960. Pollenanalytische Untersuchungen zur Vegetationsgeschichte der insubrischen Schweiz. Denkschr. Schweiz. Naturforschenden Ges. 83, 45–156.